RSC Advances

REVIEW

View Article Online
View Journal | View Issue

Cite this: *RSC Adv.*, 2018, **8**, 29428

Current advances of carbene-mediated photoaffinity labeling in medicinal chemistry

Sha-Sha Ge,[a] Biao Chen,[a] Yuan-Yuan Wu,[a] Qing-Su Long,[a] Yong-Liang Zhao,[a] Pei-Yi Wang[a] and Song Yang *[ab]

Received 24th April 2018
Accepted 7th July 2018

DOI: 10.1039/c8ra03538e

rsc.li/rsc-advances

Photoaffinity labeling (PAL) in combination with a chemical probe to covalently bind its target upon UV irradiation has demonstrated considerable promise in drug discovery for identifying new drug targets and binding sites. In particular, carbene-mediated photoaffinity labeling (cmPAL) has been widely used in drug target identification owing to its excellent photolabeling efficiency, minimal steric interference and longer excitation wavelength. Specifically, diazirines, which are among the precursors of carbenes and have higher carbene yields and greater chemical stability than diazo compounds, have proved to be valuable photolabile reagents in a diverse range of biological systems. This review highlights current advances of cmPAL in medicinal chemistry, with a focus on structures and applications for identifying small molecule–protein and macromolecule–protein interactions and ligand-gated ion channels, coupled with advances in the discovery of targets and inhibitors using carbene precursor-based biological probes developed in recent decades.

1. Introduction

The identification of targets of active molecules and natural products plays an important role in biomedical research and drug discovery. As a result of current advances in mass spectrometry and bioinformatics used in chemical probes, increasing numbers of biological targets have been found and become clinical drug candidates. However, most of them still remain unknown because there is little understanding of the mode of action between probes and relevant targets. The concept of photoaffinity labeling (PAL) was originally introduced by Frank Westheimer in the early 1960s,[1] and since then it has gradually emerged as a powerful tool for the identification and localization of targets and corresponding interaction sites in complicated biological systems,[2] especially in some cases such as low-abundance proteins and low-affinity interactions that fail to survive disruptive washing steps.[3,4] Four common types of photoreactive group are used in PAL, namely, aryl azides (AZs), benzophenones (BPs), diazirines (DAs)[5,6] (New) and 2-aryl-5-carboxytetrazoles (ACTs),[7,8] which are classified in accordance with their photochemically generated reactive species, namely, nitrenes, diradicals, carbenes and carboxy-nitrile imines. In addition, some photoreactive components of natural molecules that can undergo photolysis to form highly reactive intermediates, such as steroid enones (*e.g.*, pyrones and pyrimidones[9]), various aryl chlorides, and several thioethers, have been utilized as probes to avoid complications associated with fully synthetic probes.[10] The mechanisms of different types of photoaffinity labeling are simply illustrated in Fig. 1. In particular, carbenes are highly reactive species with extremely short lifetimes[11] that can not only react with various nucleophilic residues, but also be inserted into C–H or O–H bonds. Carbene-mediated photoaffinity labeling (cmPAL) has been increasingly used in target identification owing to the small size of carbenes, high crosslinking efficiency, long excitation wavelength, excellent chemical stability, less disruption of the interaction interface and minimal damage to biological samples. There are two major types of carbene precursor used in cmPAL, namely, diazirine and diazo compounds, which have occupied a uniquely important place in PAL. In particular, in comparison with the latter, diazirines generate relatively more reactive carbenes[12,13] and have either relatively high thermal and chemical stability[2] or a much shorter lifetime when activated by photoirradiation. The potential of carbene precursors as photoreactive groups, especially 3H-aryldiazirines with an absorption wavelength ranging from 340 to 380 nm, was first revealed in 1973 by Jeremy Knowles.[14] Since then, carbene precursor analogues of several biologically important ligands such as amino acids, nucleic acids, lipids, carbohydrates and steroids have been used as photoprobes[15] for ligand-binding sites to facilitate the formation of a covalent bond in biological systems upon photoirradiation at a certain wavelength. The boom in cmPAL, as well as the recent development of various diazirine–compatible reactions[12] and the increasing commercial availability of diazirine derivatives, has inspired equally innovative advances in research into small molecule–protein and macromolecule–protein interactions and ligand-gated ion channels. In the last few decades, a great deal of

[a]*State Key Laboratory Breeding Base of Green Pesticide and Agricultural Bioengineering, Key Laboratory of Green Pesticide and Agricultural Bioengineering, Ministry of Education, Center for R&D of Fine Chemicals of Guizhou University, Guiyang 550025, China. E-mail: jhzx.msm@gmail.com; Fax: +86-851-8829-2170; Tel: +86-851-8829-2171*

[b]*College of Pharmacy, East China University of Science & Technology, Shanghai 200237, China*

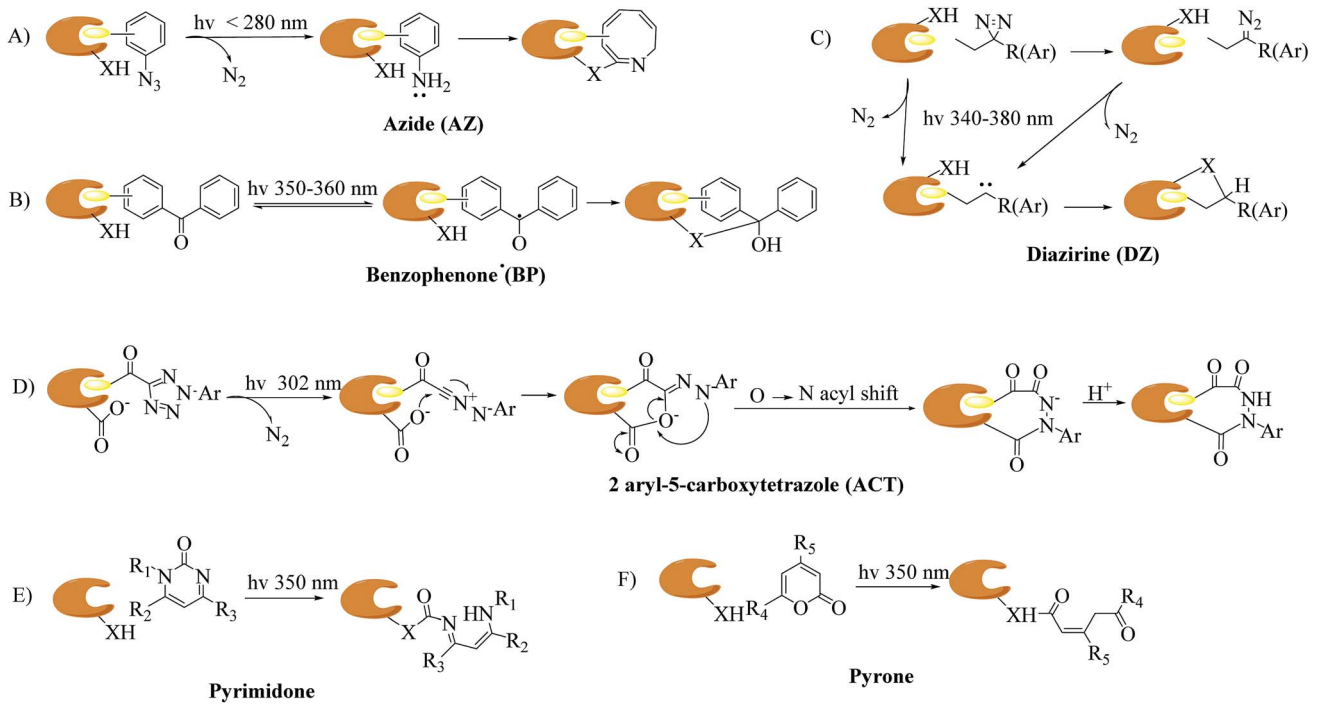

Fig. 1 Proposed mechanisms of different types of photoaffinity labeling: (A) azide (AZ), (B) benzophenone (BP), (C) diazirine (DZ), (D) 2-aryl-5-carboxytetrazole (ACT), and two "more natural" types, namely, (E) pyrimidone, and (F) pyrone. X = C, N, O, or S.

effort has been dedicated to characterizing many classes of enzymes such as kinases, γ-secretases, methyltransferases, metalloproteinases and histone deacetylases (HDACs) by using cmPAL in combination with chemical probes, namely, affinity-based probes (AfBPs), in which cmPAL is used to create covalent interactions between the probe and an enzyme that does not employ a catalytic nucleophilic amino acid within the ligand-binding site. Interestingly, a large number of these enzymes are relevant to human diseases and thus provide opportunities for the potential diagnosis and therapy of cancer.

Several excellent reviews have extensively summarized the field of cmPAL and its application in the identification of targets of natural products and bioactive compounds within the past decade.[15–20] In this highlight, we will briefly introduce current developments in cmPAL in medicinal chemistry, with a focus on synthetic methods and applications for understanding biological molecule–protein interactions and ligand-gated ion channels, as well as the discovery of targets and inhibitors using different diazirinyl biological probes that were developed recently. By presenting specific examples, we show here that cmPAL provides researchers with a distinctive set of chemical tools to embark on the study of the identification of targets of drug candidates with an unknown mode of action and the functions of many of the uncharacterized classes of enzymes that populate eukaryotic and prokaryotic proteomes.

2. Carbene-mediated PAL (cmPAL)

Carbenes are more reactive species than nitrenes with extremely short lifetimes that can not only be inserted into C–H or O–H bonds in proteins, but also react with various nucleophilic residues. As major precursors of carbenes, diazo compounds and diazirines (Fig. 2) have occupied a uniquely important place in photoaffinity labeling. Upon exposure to UV light at a certain wavelength (350–380 nm), carbenes generated by diazo compounds or diazirines are capable of spontaneously forming a covalent bond with a neighboring molecule *via* insertion into bonds such as C–H, O–H, N–H and C–C to stabilize the interaction between a biological target and a probe. The use of cmPAL in enzyme modification was first described in 1962,[1] when Westheimer *et al.* reported the use of a diazoacetyl group to inactivate chymotrypsin. Since then, there has been a steady increase in the use of cmPAL for understanding enzymes, in particular those with previously uncharacterized functions, because of its distinct advantages. The employment of both types of carbene precursor in AfBPs is illustrated below.

2.1. Diazo compounds

The diazo group has been widely used in the field of organic chemistry for over a century owing to its diverse reactivity, including alkylation, carbene generation, nucleophilic addition, homologation, and ring expansion.[21,22] Similarly, the diazo group is particularly attractive as a photoprobe and has enabled novel modifications of proteins and nucleic acids[23] (New)

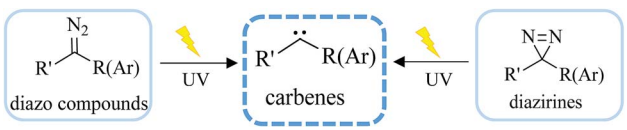

Fig. 2 Structure of carbenes derived from diazo compounds or diazirines upon UV irradiation.

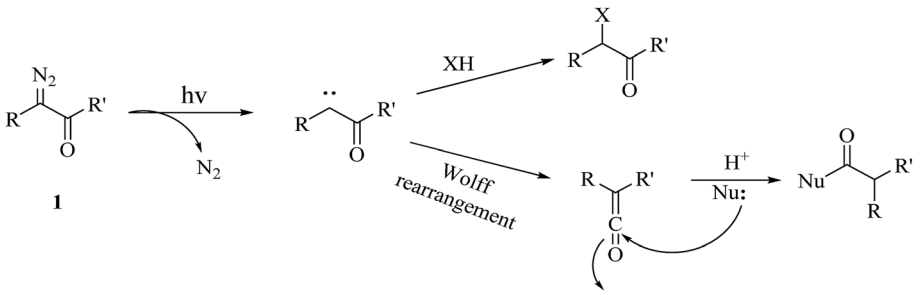

Fig. 3 Photochemical reaction of diazoketone **1** for photoaffinity labeling, including an insertion reaction and a Wolff rearrangement.

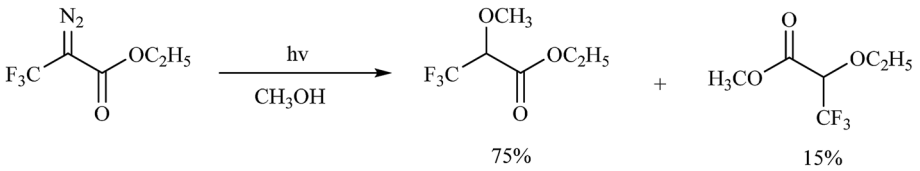

Scheme 1 Photochemical reaction of ethyl diazotrifluoropropanoate.

because of its small size and ease of introduction within a short time.[24,25] The first example of PAL was achieved with a diazoacetate.[1] Upon photoirradiation, the diazoketone **1** fragments into molecular nitrogen and a highly reactive carbene, which can undergo either a photolabeling process *via* bond insertion[26] or a Wolff rearrangement,[27] followed by nucleophilic attack on the resulting ketene (Fig. 3). Both of these products can react with neighboring functional groups and thus have a negative impact on accurate photolabeling.[13] To reduce the probability of a Wolff rearrangement and stabilize the carbene, electron-withdrawing groups can be introduced. This conclusion has been confirmed by Chowdhry *et al.*, who demonstrated that the photolysis of ethyl diazotrifluoropropanoate in methanol causes much less rearrangement and results in an efficient insertion reaction with the O–H bond (Scheme 1).[28] With high stability and a maximum UV absorption at around 360 nm, diazo compounds hold promising potential for use in photolabeling studies.[29,30] This strategy has been a powerful biochemical technique for mapping the architecture of chymotrypsin,[1] revealing antibody-binding sites,[31] examining the structure of lipid membranes,[32] and identifying isoprenoid-binding sites in proteins.[33]

The first diazo compound was synthesized in the 19th century.[34,35] As a result of their broad reactivity and coexisting functional groups, diazo compounds can present a challenge with respect to their preparation and purification. Here, we have summarized several typical synthetic methods for preparing diazo compounds (Fig. 4).[36] Among these, the preparation of diazo compounds *via* the fragmentation of triazenes was originally described by Baumgarten[37] and has been increasingly used in recent years because of its mild synthetic conditions, and thus facilitated more biological applications such as the labeling of proteins and use as tunable reactants in 1,3-dipolar cycloaddition reactions with cycloalkynes. A further effort was made by Myers *et al.*, who used azides as substrates and employed mild tetrahydrofuran–water conditions to synthesize a variety of alkyl acyl triazenes. The ability of Staudinger-type phosphines to produce diazo compounds also revealed that these acyl triazenes undergo thermal or base-catalyzed fragmentation to form α-diazo compounds in high yields.[36] Similarly, Chou *et al.* described another transformation that utilized an activated phosphinoester to convert an azide into a diazo compound in a phosphate buffer at neutral pH and room temperature. As azido groups can be easily introduced into and retained in their ligands, the conversion between azides and diazo compounds tolerates the presence of functional groups relevant to chemical biology.[38]

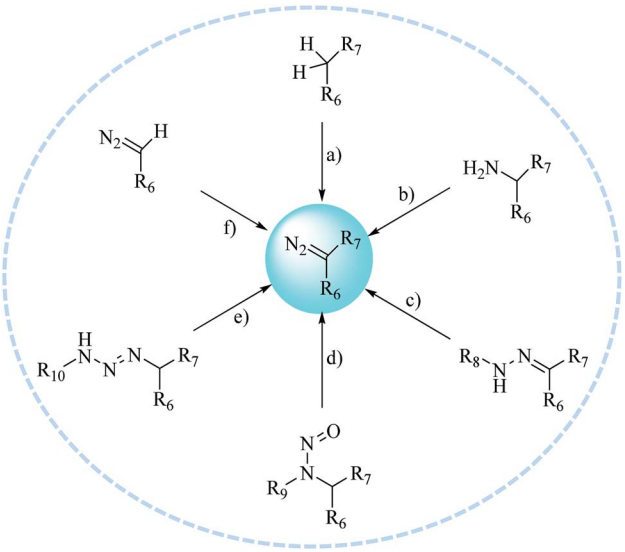

Fig. 4 Typical methods for preparing diazo compounds: (a) diazo transfer; (b) diazotization; (c) decomposition or oxidation of hydrazones; (d) rearrangement of *N*-alkyl-*N*-nitroso compounds; (e) fragmentation of 1,3-disubstituted alkyl aryl triazenes; and (f) elaboration of more readily available diazo compounds.

2.2. Diazirines

Diazirines were first chemically synthesized in 1960,[39,40] and their structures were confirmed in 1962.[41,42] A diazirine molecule is a three-membered ring system containing two nitrogen atoms and one carbon atom, which can be further categorized into two types, namely, aromatic and aliphatic compounds, depending upon whether the diazirine ring is attached directly to an aromatic ring or to an aliphatic carbon atom, respectively. Diazirines can be decomposed into molecular nitrogen and a very short-lived singlet carbene under the influence of light. In addition to generating carbenes, they can undergo isomerization to be transformed into linear diazo compounds (>30%), which also generate carbenes or carbocations for labeling the nucleophilic residues of proteins. A proportion of the highly reactive singlet carbenes immediately form a covalent bond with X–H (X = C, N, O, or S) or C–C bonds derived from a neighboring molecule *via* insertion under stable physiological conditions. The other singlet carbenes can be transformed into triplet carbenes, in which two electrons with parallel spins occupy two different orbitals *via* intersystem crossing (ISC). Singlet and triplet carbenes exhibit similar reactivity in comparison with the corresponding nitrenes. The intrinsic efficient reactivity of the singlet carbene with O–H bonds leads to scavenging of the reactive species by water. The triplet carbene is initially converted into a radical intermediate, which either undergoes an insertion reaction like the singlet carbene when it reacts with an X–H bond or abstracts a second hydrogen atom from a different C–H bond, which results in reduction. The triplet carbene can be oxidized to the corresponding ketone by molecular oxygen.[13] In summary, the reactive species in diazirine photolabeling are primarily the singlet carbene and the diazo compound, of which the proportion depends upon the chemical nature of the diazirine.[15] Another main drawback of diazirines is their complicated synthetic methods. Despite all these factors, diazirines have increasingly been employed in cmPAL as photoreactive reagents owing to their unique advantages, which include smaller sizes, longer excitation wavelengths (350–380 nm) and higher photocrosslinking efficiency than other photoreactive groups. On the other hand, in comparison with diazo compounds, diazirines generate relatively more highly reactive carbenes[12,13] and have either relatively high thermal and chemical stability[2] or a much shorter lifetime when activated by photoirradiation. Hence, diazirines have largely superseded diazo compounds as photoreactive reagents on account of their improved chemical stability in the dark and higher photochemical responsiveness. Furthermore, the recent development of various diazirine-compatible reactions,[12] coupled with the increasing commercial availability of diazirine derivatives, now allows their more widespread use in cmPAL. Diazirines have been increasingly regarded as among the most promising photolysis reagents. Attention has been given to different types of diazirinyl analogues with different biologically important ligands such as amino acids, nucleic acids, lipids, and so on, which are discussed below.

2.2.1 Aromatic diazirines. The potential of diazirines as photoreactive groups, in particular that of 3*H*-aryldiazirines (Fig. 5), was first revealed in 1973 by Jeremy Knowles.[14] Aromatic diazirine derivatives, especially trifluoromethylphenyl diazirine (TPD) derivatives,[43] in which the diazirine group is directly attached to an aromatic ring, have been developed to address some of the limitations associated with alkyldiazirines, one of which is low crosslinking efficiency because of the rapid isomerization of the photogenerated carbene intermediates into diazo isomers.[43] Furthermore, several studies have indicated that aromatic diazirines tend to photogenerate more carbenes than alkyldiazirines.[44–46] In comparison with other diazirines, TPDs display much higher chemical stability under a wide variety of conditions, including strongly acidic, strongly basic, oxidizing and reducing agents.[12] This is because the electron-withdrawing nature of the trifluoromethyl group and phenyl group located at the α-position of the diazirine moiety can not only prevent the carbene from undergoing rearrangements but also strongly stabilize the photogenerated diazo isomer under normal photolysis conditions. With a maximum absorption at around 360 nm, aromatic diazirines minimize damage to the targeted biological system. Aromatic diazirines are quite bulky in comparison with small diazirines but can be incorporated into molecules with a structure similar to that of naturally occurring compounds to address this issue; thus, the biological activity of the modified ligand and the crosslinking efficiency of cmPAL-based probes are not impaired too greatly. In general, aromatic diazirines preferentially react with O–H bonds rather than C–H bonds.[47,48] One shortcoming of TPDs is that aromatic diazirines can react with N–H bonds and generate enamines as

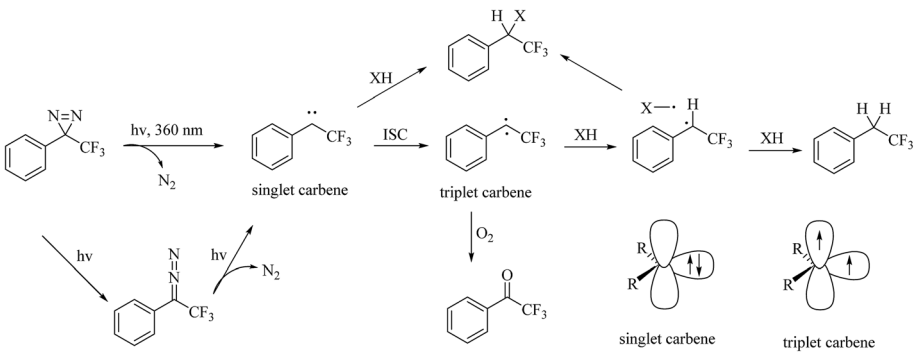

Fig. 5 Possible pathways and intermediates formed after photolysis of 3-aryl-3*H*-diazirines and representation of the electronic states of the carbene.

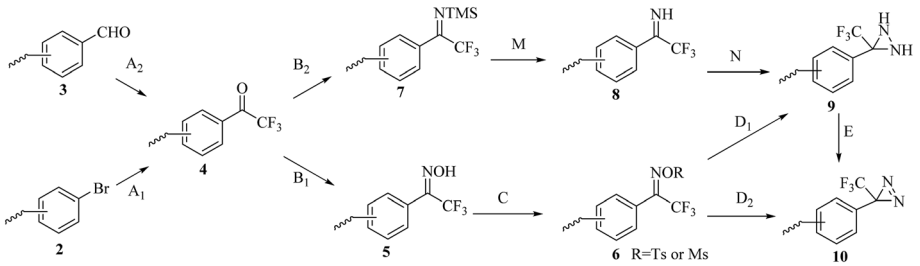

Scheme 2 Synthetic routes to the aromatic diazirine **10** from the aromatic bromide **2** or the aromatic formaldehyde **3**.

a side product, which are subject to further hydrolysis with concomitant loss of the labeling targets.[49] Collectively, TPDs are currently preferred as the most promising photolabeling reagents that have been developed, although their synthetic routes have been intricate thus far.

Although TPDs appear to be the most promising photoreactive reagents for cmPAL, their introduction into different chemical probes in a simple and convenient manner remains challenging and constitutes the major hindrance to their practical use.[2,12] A great deal of work has been invested in improving their synthesis (Scheme 2). The general strategy for preparing an aromatic diazirine analogue **10** comprises the conversion of a ketone derivative **4**, which can be obtained from an aromatic bromide **2** or an aromatic formaldehyde **3**, into the corresponding ethanone oxime **5**. The hydroxy group in **5** can be activated to form a good leaving group by using either *p*-tosyl chloride (TsCl) or mesyl chloride (MsCl) to give a tosyl oxime **6**. After treatment with NH_3 (l), the tosyl oxime **6** is converted into a diaziridine **9** and then oxidized to **10**. Another synthetic strategy includes the direct conversion of the tosyl oxime **6** into

Table 1 Summary of steps in the synthesis of aromatic diazirines. MsCl: mesyl chloride; Py: pyridine; pTsCl: *p*-tosyl chloride; DMAP: *N*,*N*-dimethyl-4-aminopyridine

Step	Synthetic conditions	Ref.
A_1	*n*-BuLi, ether, CF_3COOEt, −78 °C, 2 h	49,53
	n-BuLi, THF, CF_3COOMe, −78 °C, 2 h	54
	Mg, CF_3COR, R = piperidinyl	55
	Mg/CF_3COOH or *n*-BuLi/CF_3COR, R = OMe, piperidinyl	20
A_2	(1) TMS-CF_3, catalytic TBAF, THF; then aqueous HCl	56
	(2) Dess-Martin periodinane, TFA, CH_2Cl_2	
	(1) TMS-CF_3, K_2CO_3, DMA, rt, 2 h	57
	(2) 1 M HCl, rt, 1 h	
	(3) Dess-Martin, CH_2Cl_2, rt, 8 h	
B_1	NH_2OH, NaOH, EtOH, reflux, 21 h	49
	$NH_2OH\cdot HCl$, pyridine, EtOH, 60 °C, 4 h	53–58
	$NH_2OH\cdot HCl$, NaOH, EtOH, reflux, 16 h or pyridine, 70 °C, 3 h	59
B_2	1 M $LiN(TMS)_2$ in THF, toluene, 0 °C	51
C	MsCl, TEA	49
	TsCl, pyridine, reflux	2,53,54,56,59
	TsCl, TEA, *N*,*N*-dimethylaminopyridine, CH_2Cl_2, 0 °C, 45 min	55
	TsCl, DMAP, TEA, CH_2Cl_2, rt, 45 min	57
D_1	NH_3 (l), CH_2Cl_2, −78 °C	49,54,55
	NH_3 (l), ether, −78 °C→rt or rt	53,56,57,59
	NH_3 (l), 80 °C, 20 h	58
D_2	NH_3 (l), $LiNH_2$, rt, 11 h	50,57,59
M	MeOH, 18 h	51
N	(1) 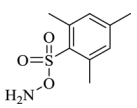 in THF, 0 °C	51
	(2) piperidine	
E	Ag_2O, ether, 23 °C, 3.5 h	49,54
	tert-BuOCl, TEA	2,55
	I_2, TEA, CH_2Cl_2 or MeOH, 0 °C	56,58,59
	MnO_2, ether or CH_2Cl_2, rt	53,57
	$(COCl)_2$, DMSO, DCM, −78 °C	60

an aromatic diazirine under the following conditions: either using liquid NH_3 at 80 °C or with $LiNH_2$ (ref. 50) (Table 1). The diaziridine can also be made using an ammonia-free synthetic method, which significantly requires less time to prepare TPDs.[51] The phenyl ketone **4** reacts with lithium bis(trimethylsilyl)amide to give an *N*-TMS-ketimine **7**, which is then subjected to solvolysis with methanol to provide an imine **8** in good yields, followed by treatment with *o*-mesitylenesulfonyl hydroxylamine, which was synthesized according to the methodology reported by Tamura *et al.*,[52] to give the corresponding diaziridine. Details of the reagents and conditions in the syntheses of the aromatic diazirine **10** are summarized in Table 1.

2.2.2 Alkyldiazirines. Increasing numbers of researchers are using alkyldiazirines for photolabeling studies, despite initial apprehensions due to their extremely small size, although TPDs appear to come closest to satisfying the chemical and biological criteria required for ideal photoprobes.[43] Typically, 3*H*-diazirine, which is the simplest form of diazirine, when the ring system has been directly attached to alkyl carbon atoms has been used to probe different states of proteins.[61–63] The use of alkyldiazirines has been limited in the past, mainly for the reasons that they are prone to generate smaller amounts of carbenes upon UV irradiation and have moderate crosslinking efficiency owing to the side products from rearrangement reaction. Furthermore, the diazo compounds derived from alkyldiazirines are liable to generate carbocations that can react with nucleophilic side chains in amino acids, which leads to non-specific photolabeling. Nevertheless, all these limitations of alkyldiazirines can be compensated for by their extremely compact sizes, which make them highly attractive in cases in which the drug–target interactions are sensitive to the size of the photoprobe. Furthermore, one of the most essential challenges in cmPAL is that the probe, which is a derivative of the drug or natural product, must retain most of the original biological activities of the original compound and exhibit little alteration in binding to the native target after modification. A smaller probe size is desirable to minimize the chance that the crosslinking group will disrupt the interaction interface and cause a significant decrease in affinity with the target molecule. This therefore calls for the development of "minimalist" linkers in which both the photoactivatable group and the detection moiety are made as small as possible so as to provide a chemically suitable modality for detecting covalent protein–probe interactions *in vivo*. Since the concept of the "minimalist linker" was first introduced by Yao *et al.* in 2013,[64] both a diazirine and a clickable moiety have been concurrently incorporated into a single alkyl chain ($\mathbf{L_{1-3}}$, Scheme 3).[64,65] This strategy has been demonstrated to be a remarkably efficient method for cmPAL and cell imaging. Very recently, a suite of "minimalist linkers" containing alkyldiazirine units and different bioorthogonal tags have been developed to find targets of BRD4 inhibitors and obtain better insights into how a tag might affect the overall performance of a probe[66] (New). In another case, a derivative of a non-steroidal anti-inflammatory drug (NSAID), namely, a photo-NSAID, containing a "minimalist linker" was used to study NSAIDs. Such a strategy not only enables the characterization of binding site hotspots for NSAIDs but can also map global binding sites for virtually any molecule of interest[67] (New).

In a similar way to aromatic diazirines, the main strategy for the synthesis of alkyldiazirines comprises starting from an aliphatic ketone, modifying it to form an alkyldiazirine and preparing diazirine precursors without oximation and tosylation. The syntheses of three commonly used alkyldiazirine-based linkers are described here. An alkyl ketone directly reacts with ammonia and an aminating reagent such as a chloramine or hydroxylamine-*O*-sulfonic acid to give the corresponding diaziridine. After oxidation of the corresponding diaziridine with a variety of oxidants, such as Ag_2O, I_2/TEA or CrO_3, the desired diazirine $\mathbf{L_1}$ is prepared (Scheme 3). In addition, a simple base-mediated one-pot reaction can also be used to prepare $\mathbf{L_1}$. It was demonstrated that the intermediate can be directly converted into the diazirine after the addition of KOH under air[68,69] (New). The synthesis of $\mathbf{L_2}$ from $\mathbf{L_1}$ was accomplished by treatment with commercially available ethyl diazoacetate and a catalytic amount of $Rh_2(OAc)_4$, and further reduction of the C-3 ester in $\mathbf{L_2}$ by DIBAL afforded $\mathbf{L_3}$ in an excellent yield[65] (Scheme 3).

3. Applications of cmPAL for biological molecule–protein interactions and ligand-gated ion channels

The chemical and thermal stability of carbene precursors allows sophisticated derivatization of the corresponding biological

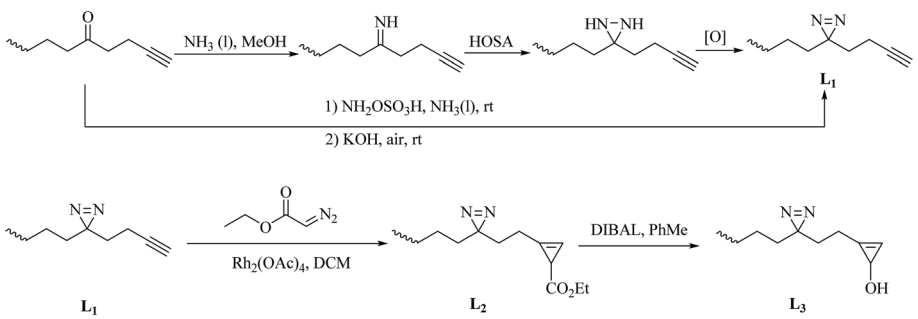

Scheme 3 Schematic of the syntheses of the minimalist alkyne linkers $\mathbf{L_{1-3}}$: HOSA: hydroxylamine-*O*-sulfonic acid; [O]: Ag_2O, I_2/TEA or CrO_3; DIBAL: diisobutylaluminium hydride.

probes, which can be further categorized according to the type of parent ligand molecule. The development of different cmPAL labels enabled a simple strategy for linking photoreactive groups, especially diazirines, to important classes of biological ligands such as amino acids, nucleic acids, lipids, carbohydrates, steroids and other small molecules to produce the corresponding diazirinyl photoprobes. Specific examples of the use of cmPAL for studying small molecule–protein and macromolecule–protein interactions and ligand-gated ion channels are discussed.

3.1. Protein–protein interactions

Because PAL can detect participants in non-covalent interactions spatioselectively, photoreactive amino acids have emerged as a critical tool for studying protein–protein interactions (PPIs) directly in a complex proteome[70] (New). The similarity between photoreactive amino acids and the corresponding natural amino acids makes them elude the stringent identity control mechanisms during protein synthesis and be directly incorporated into proteins during cell culture by the native mammalian translation machinery for protein biosynthesis.[71] Several diazirine analogues of amino acids have been widely incorporated into proteins to probe PPIs, which thereby allows the global identification of interacting proteins in living cells.

Three diazirine-containing amino acids, namely, photo-Met, photo-Leu and photo-Ile (**11–13**, Fig. 6), which resemble natural methionine, leucine and isoleucine except for the presence of a diazirine ring in the side chain, were efficiently incorporated into proteins by mammalian cells to study membrane protein complexes in living cells,[71,72] covalently detect MH2–MH2 domain interactions in proteins,[73] inhibit the expression of a vascular cell adhesion molecule (VCAM) in a fungal cyclodepsipeptide,[74] and map the protein interaction network of human protein kinase D2 (PKD2), which is an enzyme that belongs to the family of serine/threonine kinases and is involved in multiple biological processes.[75] It was demonstrated that insights from structural proteomics can be used to generate CaM-insensitive mutants of targets of CaM for functional studies *in vitro* or ideally *in vivo via* the incorporation of synthetic photo-Met.[76]

In another study, a derivative of L27-11 containing photo-Pro (**14**, Fig. 6) was reported to label LptD, which is an outer-membrane protein widely distributed in Gram-negative bacteria, against *Pseudomonas aeruginosa*[77] and enable the study of its essential function in the bacterium.[78] Similarly, two proline-based diazirinyl amino acids, namely, JB-95 (ref. 79) and DYN5,[80] were developed to study several β-barrel OM proteins, including BamA and LptD,[79] and find the potential target, which was found to be the sensor ParS.[80]

Another synthetic amino acid with a trifluoromethyldiazirine moiety attached to phenylalanine, namely, Tmd-Phe (**15**, Fig. 6), was first prepared by Nassal in 1984.[81] After the successful identification of calmodulin (CaM) using Tmd-Phe in a calcium-dependent manner,[82] Tippmann *et al.* extended the use of Tmd-Phe to label the amber codon, which gave a highly efficient and precise response in *E. coli*.[83] In a subsequent study, in order to find novel complexes of proteins with Grb2 and map PPIs in living cells, Tmd-Phe was incorporated into multiple sites (N103-L112) in the SH2 domains of Grb2 (ref. 84) and was specifically crosslinked with EGFR after stimulation by EGF.[85] In addition, some Tmd-Phe derivatives also have sufficient affinity for the sweet taste receptor to identify the binding sites of ligands in the sweet taste receptor.[86]

Photo-Trp (**16**, Fig. 6) is a new photoactivatable amino acid designed to be incorporated into tryptophan-containing peptides for cmPAL. Two types of photo-Trp, namely, 5- and 6-trifluoromethyldiazirinyltryptophan, acted as skeletons for the comprehensive synthesis of various bioactive indole metabolites and were used in biological functional analysis *via* cmPAL.[87] Furthermore, a Boc-protected version of photo-Trp, which carried a diazirinyl substituent at the 6-position of the indole ring, was used to target the cytotoxic marine natural product hemiasterlin.[88]

Two lysine-based diazirinyl analogues (**17** and **18**, Fig. 6) were developed to efficiently photocrosslink a test model protein *in vitro* and *in vivo*[89] and identify proteins that recognize PTMs of lysine, including 'readers' and 'erasers' of histone modifications,[90] respectively. In another case, genetically encoded photo-lysine was used as an unmodified "control probe" in conjunction with the photoaffinity label crotonyllysine to study the specificity of an effector of interest toward the corresponding PTM of lysine, which enabled the investigation of PPIs mediated by the lysine PTM between the full-length H3 protein and its epigenetic regulatory effectors.[91]

From these studies, we can see that the development of new photoreactive amino acids of which the structures and properties closely resemble those of natural amino acids may help to address difficulties in the identification of PPIs in living cells.

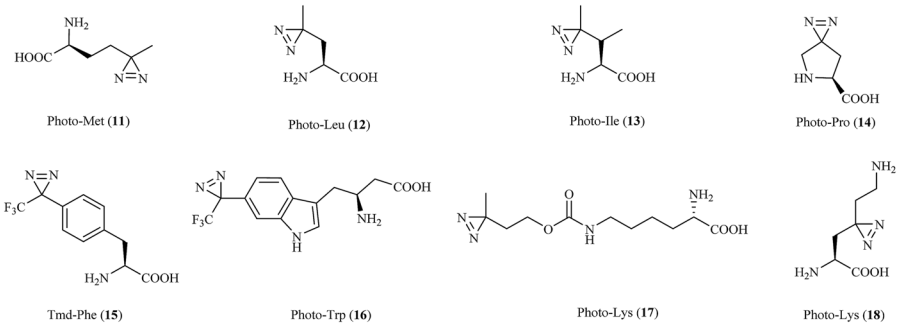

Fig. 6 Diazirine analogues of amino acids.

3.2. Nucleic acid–protein interactions

Since nucleic acid analogues that carried a diazirine unit were successfully used for cmPAL, increasing numbers of photolabile nucleoside, nucleotide and oligonucleotide analogues containing diazirines have been developed for studying nucleic acid–protein interactions.

The simplest nucleoside derivative **19** (Fig. 7), which consisted of deoxyuridine substituted at the 5-position with a 3*H*-diazirine group, was synthesized by Taranenko *et al.*, who used this so-called "zero-length" diazirinyl nucleoside to investigate nucleic acid–protein interactions.[92] In addition, two nucleotide compounds comprising cytosine (C*, **20**, Fig. 7) and guanine (G*, **21**, Fig. 7) with diazirine units were developed by He *et al.*, who described a simple and rapid solid-phase synthetic method for the incorporation of diazirine into the major and minor grooves of DNA for efficient photocrosslinking to proteins.[93] Similarly, a diazirine-based nucleoside analogue **22** (DBN, Fig. 7) was successfully incorporated into DNA by solid-phase oligonucleotide synthesis, efficiently formed inter-strand crosslinks in dsDNA upon photoirradiation and thus enabled a wide range of applications in biotechnology, such as probing nucleic acid–nucleic acid and protein–nucleic acid interactions and in phototherapy.[94] A different application of photolabile nucleic acids was described by Carell *et al.*, who synthesized two thymidine analogues **23** and **24** (Fig. 7) by attaching TPD groups to the 5-position of the nucleobase uridine to avoid disturbing the duplex structure of DNA. After cmPAL, two DNA repair enzymes (Rad14, which is the yeast homologue of human XPA protein, and Fpg/MuM-DNA glycosylase from *Lactococcus lactis*) were identified,[95] and an optimal photocrosslinker that exerted a significant effect on the yield and efficiency of photocrosslinking in the human nuclear proteome was found to be involved in processing the lesion,[96] respectively.

Several derivatives that bear a diazirine ring at different positions in RNA have been synthesized, and their photoaffinity efficiencies have been tested. Protocols for the synthesis and photocrosslinking of diazirine-containing RNAs have been described by Sergiev *et al.*, who chose *Escherichia coli* ribosomes as a model for testing photoactivated RNA analogues **25–27** (Fig. 7), which can be incorporated into RNA by T7 transcription.[97–99] The TPD moiety in the nucleotide analogue **25** is located in the major groove of the mRNA helix and is in contact with ribosomal 16S RNA in helix region 28.[97] Upon UV irradiation, the 4-thiouridine (s^4U) analogue **26** was non-specifically crosslinked to either single- or double-stranded RNA regions, which enabled an understanding of the structure and function of 5S rRNA and its environment in the ribosome.[98] The 6-thioguanosine diazirinyl analogue **27** was crosslinked at the 3′-end

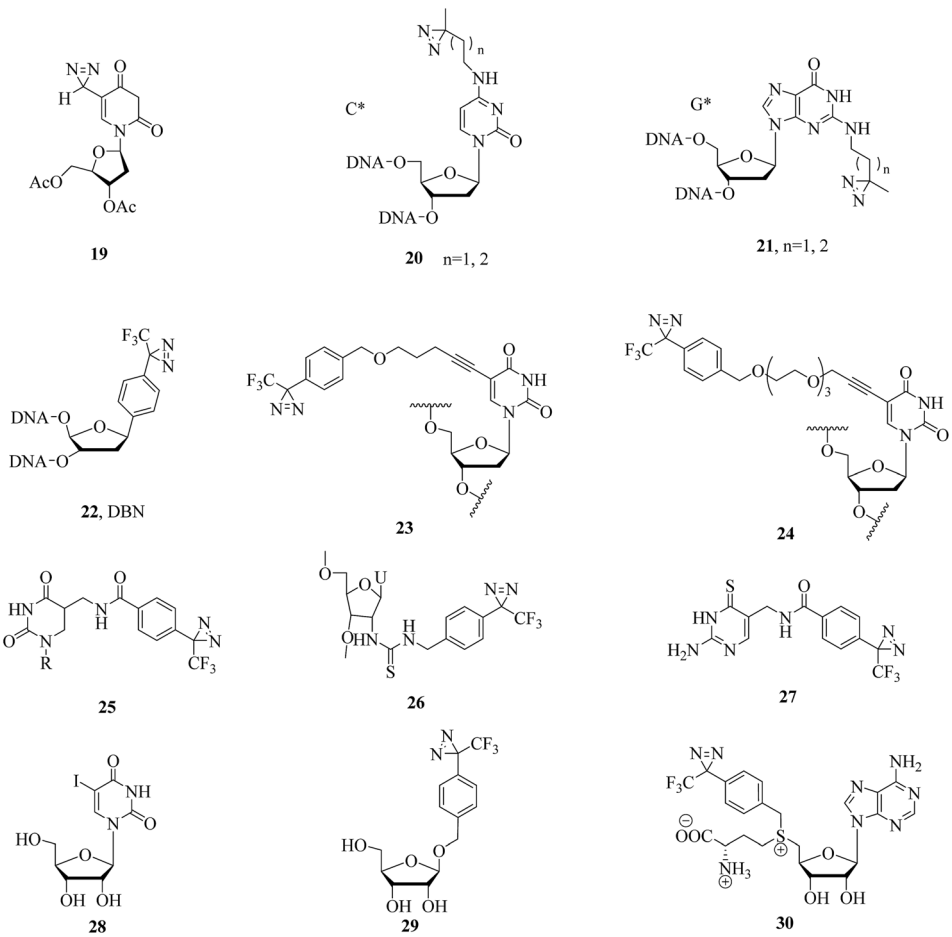

Fig. 7 Structures of diazirinyl nucleic acid analogues and the 5-iodouridine RNA derivative **28**.

of 16S rRNA (nucleotides 1496–1542), which performed photochemical crosslinking within the *E. coli* ribosome complex.[99] In another study, some photolabeled siRNAs (small interfering RNAs) with TPD moieties in the 3′-overhang region were reported and compared to a 5-iodouridine RNA derivative **28** (Fig. 7) by Ueno *et al.*, which enabled much more sensitive detection and would serve as a powerful tool for understanding the mechanism of the assembly of the RISC (RNA-induced silencing complex) by Argonaute proteins.[100] Similarly, a photoreactive miRNA-145 probe **29** containing photolabeled microRNA (Fig. 7), which has sufficient gene-silencing activity even if the guide strands of the miRNAs are modified with the analogue **29** in some cases,[101] was found to specifically label the target mRNAs, namely, FSCN1 and KLF4, upon UV-A irradiation in DLD-1 human colon cancer cells.[102] An *S*-adenosyl-L-methionine (AdoMet) analogue **30** (Fig. 7), which can be enzymatically transferred to the target of methyltransferase, namely, the mRNA cap, with high efficiency, was demonstrated to be the optimal photochemical reagent for enzymatic transfer and photocrosslinking to a directly interacting protein.[103]

These photolabeled nucleic acid analogues, in combination with cmPAL and mass spectrometry methods, should enable more scientists to characterize proteins that are specifically involved in DNA or RNA processes in detail.

3.3. Lipid–protein interactions

Diazirine analogues of lipids that bear photoreactive diazirine groups in either the polar head or the hydrophobic part can be incorporated into a lipid bilayer to study lipid–protein interactions. When exposed to light, photogenerated highly reactive carbenes can covalently crosslink with membrane proteins or surrounding lipids. Since the first aliphatic diazirine-based phospholipid was reported by Khorana *et al.* in 1980,[104] various hydrophobic diazirinyl analogues of lipids have been developed for labeling hydrophobic biomembrane regions owing to their higher labeling efficiency in hydrophobic environments in comparison with an aqueous medium.[12,105]

A pioneering study by Ross using diazirinyl lipid analogues **31**–**33** (Fig. 8) bearing diazirine groups either in the fatty acyl chain or in the polar head provided a direct method for investigating the biomembrane of glycophorin A. Further results of labeling using the phospholipid **31** showed that the Glu-70 residue is embedded in the membrane.[106] In addition, in combination with radiolabeling, two lipid analogues **34** and **35** containing TPD units (Fig. 8) were designed to study the interactions between the influenza virus and target membrane lipids,[107] mitochondrial proteins and phosphatidylcholine.[108] The successful confirmation that the HA2 subunit of influenza hemagglutinin was inserted into the target membrane prior to fusion[107] and the highly specific

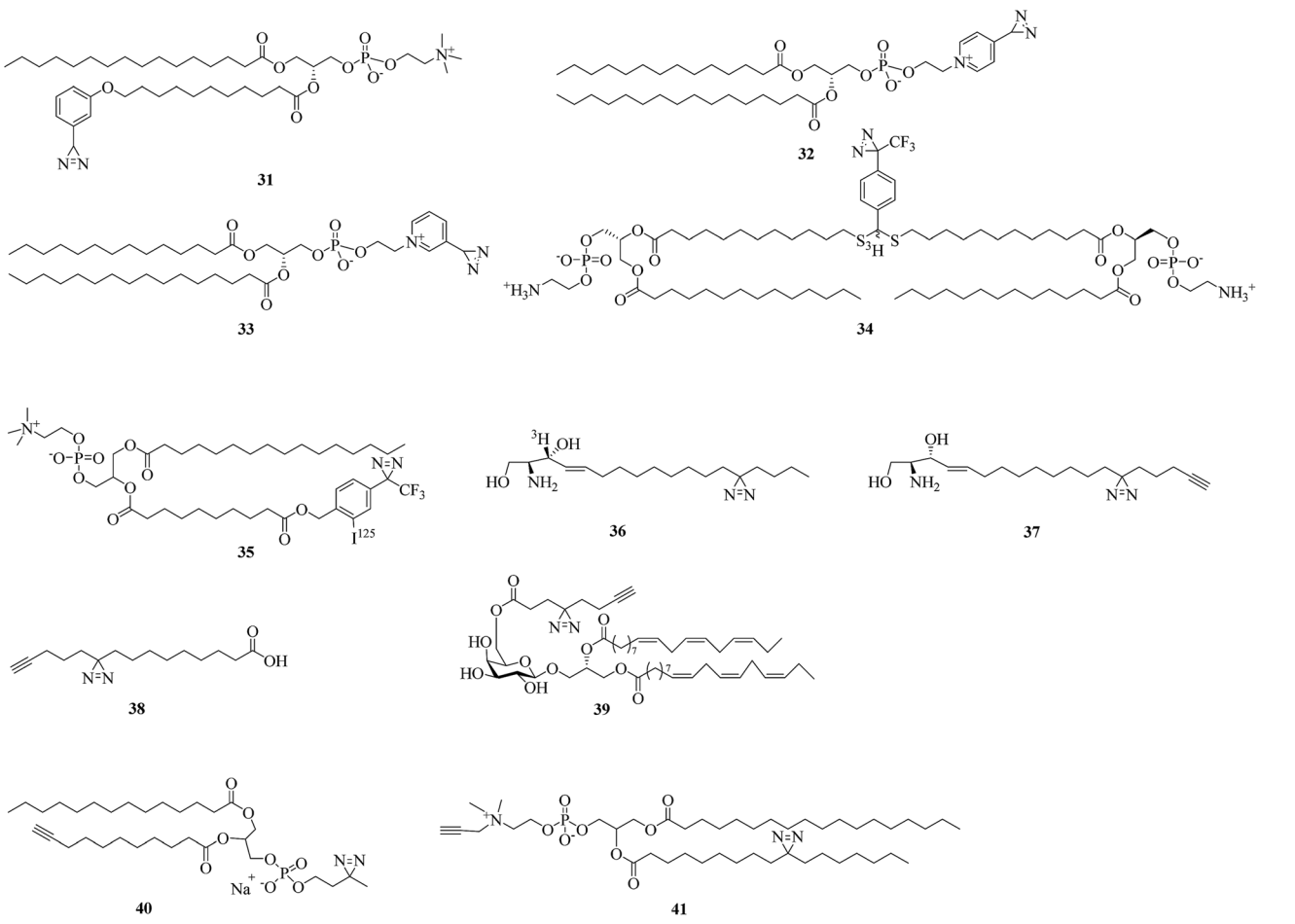

Fig. 8 Diazirine analogues of lipids.

labeling of a 70 kDa protein[108] indicated the potential of these two photolipid analogues as tools for proteome analysis.

As structural components of membranes, sphingolipids can act as intracellular second messengers. In order to understand how sphingolipids affect the function of proteins within the membrane bilayer of living cells, Haberkant *et al.* developed a radioactively labeled photosphingosine **36** (Fig. 8)[109] and two clickable photosphingosines **37** (Fig. 8)[110] and **38** (Fig. 8)[111] bearing an alkyldiazirine moiety in the fatty acyl chain. A bifunctional sphingosine such as **38** can not only be metabolically incorporated into all major classes of glycerolipids, as well as into proteins *via* fatty acylation in living cells, but can also be conjugated to a coumarin caging group *via* a carbamate linkage at the amino group to give a trifunctional sphingosine for studying different aspects of lipid biology in the context of living cells.[112] Another clickable fatty acid-based probe **39** (Fig. 8) was reported by Liu *et al.*, who designed a fatty acid-based probe bearing diazirine and terminal alkyne groups, which enables the identification or visualization of the respective crosslinked protein–glycolipid complex.[113]

Similarly, in order to discover more new protein–lipid interactions in which proteins bind to phosphatidylcholine (PC), which is the most abundant type of phospholipid in most lipoproteins and membranes, *via* the fatty acid tails, two photoactivatable and clickable phosphatidylcholine analogues **40** and **41** (Fig. 8) were prepared.[114,115] Compound **40**, which can be incorporated into recombinant high-density lipoprotein particles or membrane bilayers, facilitated the identification of residues critical for the docking of proteins with the lipid surface of lipoproteins or cell membranes.[114] The other PC analogue **41** was used in a double incorporation strategy for the metabolic synthesis of bifunctional PCs to provide an obvious improvement in global mapping of genuine protein–lipid interactions in living cells. It is evident that this strategy not only facilitates the successful biosynthesis of bifunctional **41** but also identifies many high-confidence PC-binding proteins.[115]

It is evident that alkyldiazirine analogues of lipids bearing diazirines in the fatty acyl chain have been increasingly used to study protein–lipid interactions in biological membranes in recent years owing to their smaller size and close structural resemblance to lipid derivatives.

3.4. Carbohydrate–protein interactions

Carbohydrates constitute integral components of the cell machinery in the forms of polysaccharides, proteoglycans, glycoproteins, glycolipids, and glycosylated secondary metabolites and play crucial roles in a wide range of biological and pathological processes.[116] However, there are still many carbohydrate–protein interactions that remain unknown owing to transient and low-affinity interactions.[117] The use of carbene-mediated photocrosslinking of sugars represents a powerful strategy for investigating carbohydrate–protein interactions in their native context. Several efforts have been made to develop diazirinyl carbohydrate analogues to provide the first step in elucidating the biological roles of carbohydrates.

In a related study, Kuhn *et al.* prepared two thioglycoside carbohydrate analogues **42** (Fig. 9)[118] and **43** (Fig. 9)[119] bearing a diazirine photoreactive group for photocrosslinking β-galactosidase and β-hexosaminidase, respectively. Under UV light, the group can generate a reactive carbene that can undergo an insertion reaction with a nearby amino acid residue within the enzyme. A tritium label [^{3}H] was used to radiolabel the captured target. Similarly, a diazirinyl carbohydrate analogue [^{3}H]-1-ATB-GalNAc **44** (Fig. 9), in which the R group was replaced by an acetamide group, has been employed as a useful photocrosslinking reagent to label Glu-355, which is highly conserved and located within a region of Hex B.[120]

A great deal of effort has been made by Kohler *et al.*, who designed and synthesized a series of diazirine-containing photosugars, typically, a sialic acid analogue SiaDAz (**45**, Fig. 9) and an *N*-acetylmannosamine analogue ManNDAz (**46**, Fig. 9), which were metabolically incorporated into cell surfaces for the covalent detection of transient interactions between sialic acids and sialic acid-recognizing proteins *via* cmPAL. With the help of a commercially available sialidase that removed the natural sialic acid Neu5Ac from cell surfaces while leaving SiaDAz-modified glycoconjugates intact, the utility of SiaDAz was greatly improved, and this process can be applied generally in the case of sialic acid-mediated interactions and will facilitate the identification of binding partners of sialic acid.[121] In addition, a fully acetylated sialic acid photosugar Ac_5-SiaDAz (**47**, Fig. 9) and a mannosamine precursor Ac_4-ManNDAz (**48**, Fig. 9) bearing a diazirine photocrosslinker on the *N*-acyl (C-5) side chain[122] were metabolically incorporated into cell surface glycoconjugates to identify and characterize the binding partners of the glycoconjugates.[123] These two photosugars **47** and **48**, as well as the control molecule, namely, the *N*-acetylglucosamine analogue Ac_4-GlcNDAz (**49**, Fig. 9), displayed improved membrane permeability and produced photoreactive sialyl glycans in various types of cell. To demonstrate the photocrosslinking utility of these metabolically incorporated photosugars, the sialic acid-dependent oligomerization of CD22 was examined. After cells were cultured with either ManNDAz or 5-SiaDAz, photocrosslinking of CD22 was observed, whereas the control was not crosslinked, which confirmed that the crosslinking depended on the incorporation of 5-SiaDAz.[122] Using a similar metabolic labeling approach, cultured cells were induced to produce a modified nucleotide sugar donor UDP-GlcNDAz **50** (Fig. 9) and to transfer Ac_4-GlcNDAz **49** to proteins that are normally modified with an O-GlcNAc group. Subsequent photocrosslinking resulted in the selective covalent capture of O-GlcNDAz-modified nucleoporins and nuclear transport factors, which indicated that modification with an O-GlcNAc group is intimately associated with the recognition events that occur during nuclear transport.[124] Another two diazirine-modified ManNAc analogues **51** and **52** (Fig. 9) were synthesized, in which the number of methylene groups separating the carbonyl and diazirine groups in the *N*-acyl side chain was varied in order to guarantee an optimal distance for the efficient capture of binding partners of sialoside. The smallest diazirine-modified sialic acid precursor **48** was shown to be very efficiently metabolized and competed well with endogenous sialic acid.[125]

As a model carbohydrate ligand, lactose is known to bind to peanut agglutinin (PNA, K_d = 770 μM), which belongs to the lectin family of carbohydrate-binding proteins. A set of lactose-

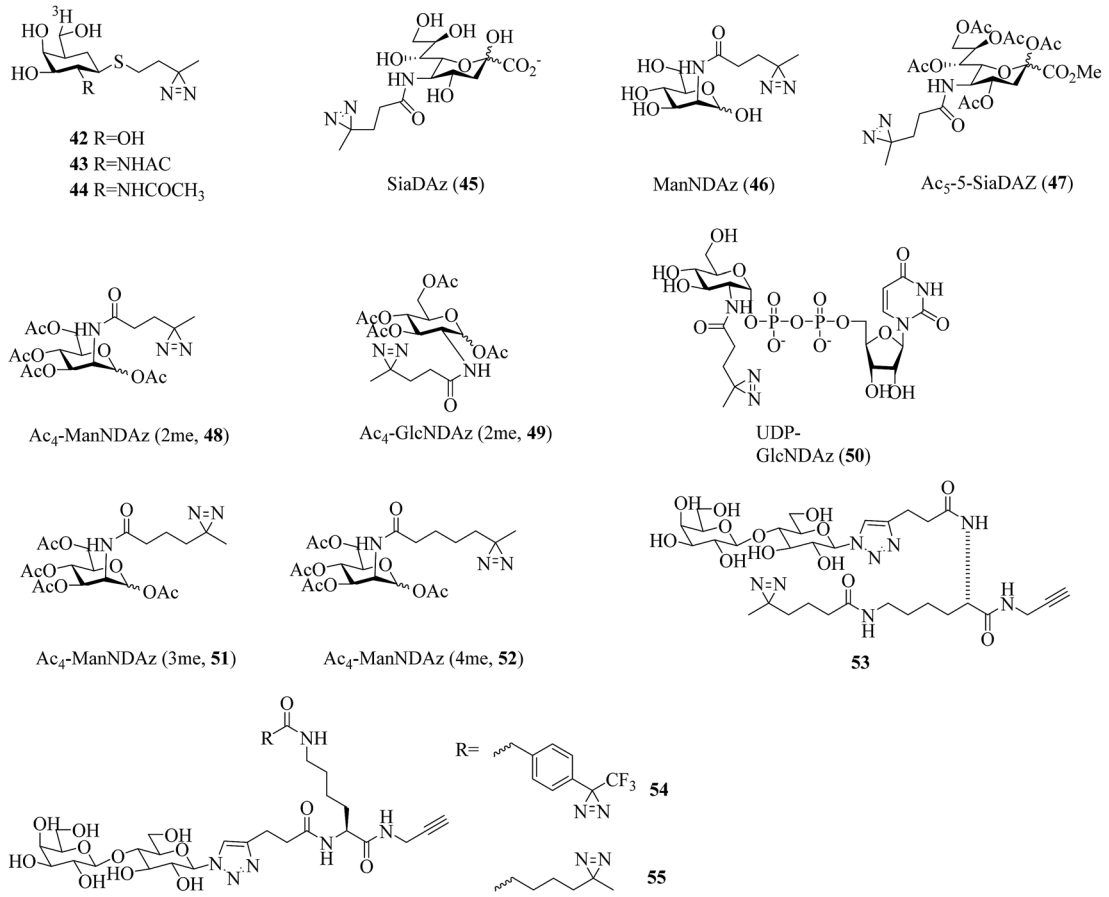

Fig. 9 Diazirine analogues of carbohydrates.

based analogues bearing different photoreactive groups, such as aryl azide, benzophenone, alkyldiazirine and trifluoromethylphenyldiazirine (TPD), were synthesized to directly compare their efficiency and selectivity in photocrosslinking a carbohydrate-binding protein. Despite the low yield of crosslinking, the diazirinyl lactose analogue (**53**, Fig. 9) displayed high ligand-dependent reactivity that was consistent with the ideal mechanism of PAL.[126] Although the crosslinking efficiency of the TPD derivative (**54**, Fig. 9) was higher than that of the alkyldiazirinyl derivative (**55**, Fig. 9) when it reacted with a single binding protein, the latter exhibited significantly more selective PAL of a binding protein in a cell lysate than the corresponding TPD derivative.[127]

In summary, diazirine analogues of carbohydrates can be metabolically incorporated into a cell surface and further used to covalently detect carbohydrate–protein interactions upon UV irradiation or as model ligands to compare different photocrosslinkers.

3.5. Steroid–protein interactions

Several photolabile steroid analogues that incorporate diazirines into the tetracyclic steroid nucleus have been developed over the past decade.

Typically, a radiolabeled diazirinyl analogue of a bile salt **56** (Fig. 10), which belongs to a class of important endogenous metabolites that consist of a steroid core and a side chain with a carboxyl group,[128] was reported to detect virtually all bile salt-binding receptors[129] and was used to investigate the taurocholate transport system in hepatocytes.[130] Similarly, another photolabile bile acid derivative **57** (Fig. 10)[131] and its analogue **58** (Fig. 10)[132] with a diazirine group attached at the 3-position of the steroid nucleus were synthesized to minimize the possibility that any receptor sites might elude detection[131] and to map proteins that interact with bile acids and are involved in many important physiological processes.[132]

More efforts have been made to study cholesterol, which is a precursor of steroid hormones and bile acids and is necessary for the functional activity of several membrane proteins. Two photoactivatable cholesterol analogues **59** and **60** (Fig. 10), in which the hydrogen atom at C-6 was replaced by a diazirine moiety, were developed to investigate cholesterol-binding proteins in neuronal cells[133] and study oxysterol-binding protein-related proteins (ORPs).[134] The results obtained by photocrosslinking showed that synaptophysin was a major specific cholesterol-binding protein in PC12 cells and brain synaptic vesicles,[133] and the strengths of the signals obtained for different ORPs do not necessarily reflect the order of their relative affinities for native 25OH.[134] In another study, a cholesterol analogue **61** (Fig. 10) was demonstrated to be an effective reagent for studying cholesterol–protein interactions

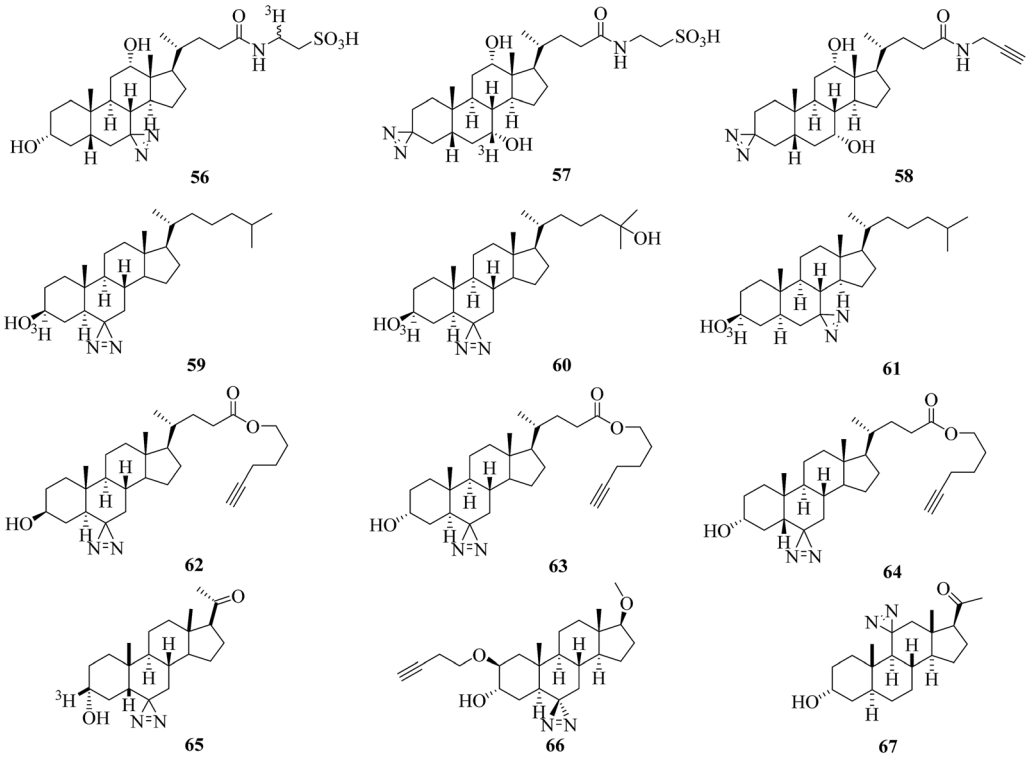

Fig. 10 Diazirine analogues of steroids.

involved in intracellular cholesterol trafficking[135] and can be used to label Niemann-Pick type C (NPC) 1 protein, which plays important roles in transporting cholesterol and other lipids out of late endosomes by means of vesicular trafficking.[136] Similarly, more than 250 cholesterol-binding proteins in HeLa cells were identified using three clickable diazirinyl sterol analogues **62–64** (Fig. 10), which differ in the diastereomeric relationship between the C-3 alcohol group and C-5 hydrogen atom attached to the cholesterol core.[137]

In other cases, in order to understand the mode of action of a neurosteroid produced from cholesterol, three photolabile neurosteroid analogues **65–67** (Fig. 10) were described.[138–140] By using the radiolabeled analogue **65** in which a diazirine moiety is attached to the C-6 position, the protein VDAC-1 was successfully identified as a neuroactive steroid-binding protein in the rat brain that may modulate the function of the $GABA_A$ receptor.[138] With a similar structure to **65**, the clickable analogue **66** exhibited selective compartmentalization in the Golgi apparatus with a preferential effect on proximal inhibition.[139] The C-11-modified photoprobe **67**, which exhibited potency equal to or higher than that of alphaxalone as a general anesthetic and potentiator of $GABA_AR$ responses, was used to discover neuroactive steroid–$GABA_AR$ binding sites.[140]

All in all, these diazirinyl steroid analogues can be used to globally map steroid–protein interactions directly in living cells. The possibility that any receptor sites will elude detection can be minimized by attaching the photolabile diazirine group at different positions in the molecule.

3.6. Ligand-gated ion channels

Propofol (Fig. 11) is the most commonly used sedative-hypnotic drug for difficult procedures and acts by potentiating $GABA_A$ (γ-aminobutyric acid type A) receptors, but where it binds to these receptors is not known. A set of propofol-based photolabeling reagents bearing diazirine moieties have been developed to identify its potential binding sites over the past decade.

In a related study, a propofol analogue *m*-azipropofol (AziPm, **68**, Fig. 11), which contained an alkyldiazirine group in a *meta*-position relative to the hydroxyl group, was synthesized to identify targets and thereby mechanisms of propofol. This design not only precluded any possible intramolecular reaction of the reactive site with the phenolic hydroxyl group but also revealed a previously identified propofol-binding cavity.[141] A further application was described that [^{3}H]AziPm was used to identify propofol-binding sites in *Torpedo* nAChR (nicotinic acetylcholine receptors), which are members of the Cys-loop superfamily of pentameric ligand-gated ion channels and can be inhibited by propofol.[142,143] After photocrosslinking, three binding sites in the transmembrane domain of nAChR, namely,

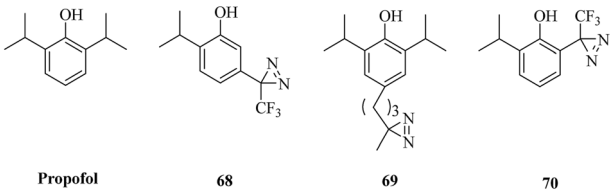

Fig. 11 Structures of propofol and its diazirinyl analogues.

the subunit helix bundle, ion channel and γ–α interface, were revealed.[144] In comparison with AziPm **68**, another photoactivatable propofol derivative *p*-4-AziC5-Pro (**69**, Fig. 11), which keeps the core structure of propofol intact by adding a reactive diazirine group at the *para*-position of the phenol ring, has different photoselectivity for amino acid residues and enables the possibility of studying the binding sites of propofol in more detail.[145] In addition, an *ortho*-propofol diazirine analogue (*o*-PD, **70**, Fig. 11) bearing a photoreactive group at the *ortho*-position of the phenol ring was synthesized to reveal unknown propofol-binding sites in membrane receptors and provides the ability to use a combination of deuterated and protiated variants of *ortho*-propofol diazirine. In combination with cmPAL, as well as high-resolution MS, a new binding site of propofol in $GABA_A$ receptors that consisted of both β_3 homopentamers and $\alpha_1\beta_3$ heteropentamers was identified.[146]

In a similar way to propofol, which acts by interacting with GABA type A receptors ($GABA_ARs$), several etomidate (Fig. 12)-based diazirine analogues, including azi–etomidate **71** (Fig. 12),[147,148] TDBzl–etomidate **72** (Fig. 12)[149] and *p*TFD–etomidate **73** (Fig. 12)[150] were synthesized by Cohen *et al.* to identify binding domains in a ligand-gated ion channel[147,149,150] and directly photolabel amino acids that contribute to an anesthetic-binding site in $GABA_AR$.[148] Photoaffinity labeling established that the analogue **71** identified two labeled amino acids, of which one was located in the membrane-spanning helix of α-subunit M1 (αMet236) and the other in the membrane-spanning helix of β-subunit M3 (βMet286).[148] It was demonstrated that the agent **72**, which contains a TPD moiety, not only exerts pharmacological actions on members of the Cys-loop ion channel superfamily of receptors[149] but also acts as a positive allosteric modulator of nAChR rather than as an inhibitor,[151] and site-directed mutagenesis suggests that S-TFD-etomidate acts at different sites in comparison with R-etomidate.[150]

Photoactivatable propofol analogues that have an alkyldiazirine moiety at different positions of the phenol ring would present a more comprehensive view of the mechanism of propofol with membrane receptors. Furthermore, these different diazirinyl anesthetic analogues would provide a powerful tool for understanding the modes of action of the anesthetic on ligand-gated ion channels.

Most of the carbene precursor analogues described here retained similar or even better biological activity in comparison with the parent compounds, largely owing to the extremely small size of the diazirine photoreactive groups and the rational selection of the positions where these photolabile groups were incorporated within the probe. Despite the sophisticated derivatization of these biological probes, the minimal interference with the original biological activity, as well as the native interactions, makes them a robust tool for studying protein–protein, protein–lipid, protein–macromolecule, protein–steroid and other ligand–receptor interactions.

4. Applications of cmPAL for discovery of targets and inhibitors

Within the past two decades, activity-based protein profiling (ABPP) *via* the employment of irreversible chemical probes has been pursued as a useful strategy for studying the subcellular location and activities of many classes of enzymes.[152–155] However, all of these must be active enzymes that contain a catalytic nucleophilic amino acid residue. In the case of low-affinity interactions between probes and inactive enzymes, the labeling usually fails to survive disruptive washing steps. The emerging technique of PAL, especially cmPAL in combination with chemical proteomics, does not necessarily label active enzymes and thus overcomes the limitations of non-covalent affinity reagents. With excellent photolabeling efficiency, minimal steric interference and longer excitation wavelengths, cmPAL when coupled with chemical probes has been increasingly developed to study various classes of enzymes and their inhibitors. Here, we introduce different applications of cmPAL for classes of enzymes and their inhibitors, including kinases, γ-secretase, methyltransferases, metalloproteinases, histone deacetylase, and so on.

4.1. Kinases

Kinases, especially protein kinases (PKs), are one of the most important classes of enzymes in human cells, play a key role in signal transduction and regulate a variety of cell processes. Of the more than 500 known PKs, many are potential therapeutic targets.[156] To study potential cellular targets of kinases and their inhibitors, recent efforts have focused on cmPAL using a large panel of AfBPs, as well as mass spectrometry-based chemical profiling methods.

As a prototypical natural-product kinase inhibitor that competes with ATP, staurosporine can target at least 253 kinases.[157] Significant efforts have been made by Yao *et al.*, who developed a staurosporine-based clickable probe STS-1 (**74**, Fig. 13) bearing a diazirine group that was capable of proteome-wide profiling of potential cellular targets in live HepG2 cells for the first time.[158] The same strategy was used to study dasatinib,

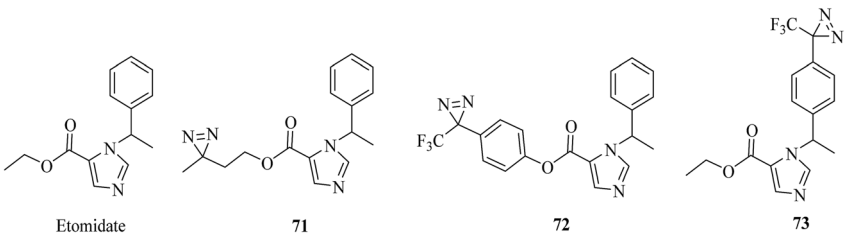

Fig. 12 Etomidate and its diazirinyl analogues.

which is a dual Src/Abl inhibitor and a promising therapeutic agent with oral bioavailability. By using the cell-permeable probe DA-2 (**75**, Fig. 13), as well as chemical proteomics methods, a number of previously unknown targets of dasatinib, including several serine/threonine kinases, were identified.[159] In addition, since improved minimalist photocrosslinkers that possess two carbon atoms on each side of the diazirine ring flanked by a terminal alkyne and a functional group (CO_2H/NH_2/I) were first introduced into 12 well-known kinase inhibitors for cell-based proteomic profiling of potential cellular targets under native conditions,[64] more potential targets of kinases have been found by using these minimalist alkyldiazirine alkyne linkers. Typically, photoaffinity probes **76** and **77** (Fig. 13) that contain a ''minimalist'' linker were capable of both live-cell imaging of the activities of aurora kinase A (AKA) and *in situ* proteomic profiling of potential off-targets of MLN8237, which is a highly potent and presumably selective inhibitor of AKA[160] and can be used to study the mechanism of action of H8, which is an inhibitor of protein kinase A (PKA).[161]

An important signal transduction protein, namely, protein kinase C (PKC), has been proposed as the target of anesthetics such as alcohols and halothane. In a similar way to these, azialcohols such as 3-azioctanol, 7-azioctanol and 3-azibutanol (**78–80**, Fig. 13) can be used for photolabeling with PKCδC_1B (the high-affinity phorbol-binding subdomain)[162,163] and locate binding sites in adenylate kinase, which is an enzyme that catalyzes the transfer of a phosphoryl group.[164] A TPD-based oleic acid probe **81** (Fig. 13) is also a useful tool for elucidating the functions of the specific activation of PKC by oleic acid.[165]

Much progress has been made in understanding the mode of action of serine/threonine kinases, which are involved in multiple cellular functions and pathological processes. In a sophisticated study, two thiol photoaffinity linkers **82** and **83** (Fig. 13) were synthesized to find the site where p62, which plays important roles in proteasomal or autophagosomal protein degradation, binds to p38, which is a serine/threonine kinase. Surface plasmon resonance (SPR) signals produced by the interaction between p38 and peptides derived from p62 were clearly detected, which enabled us to identify the binding site.[166] Another important serine/threonine kinase, namely, protein kinase D2 (PKD2), was studied using two diazirine-modified photo-amino acids **11** and **12** (illustrated in Fig. 6), as well as a series of proteomics approaches such as cmPAL, trypsin digestion and label-free LC/MS analysis, which revealed several interaction partners, to map the protein interaction network of

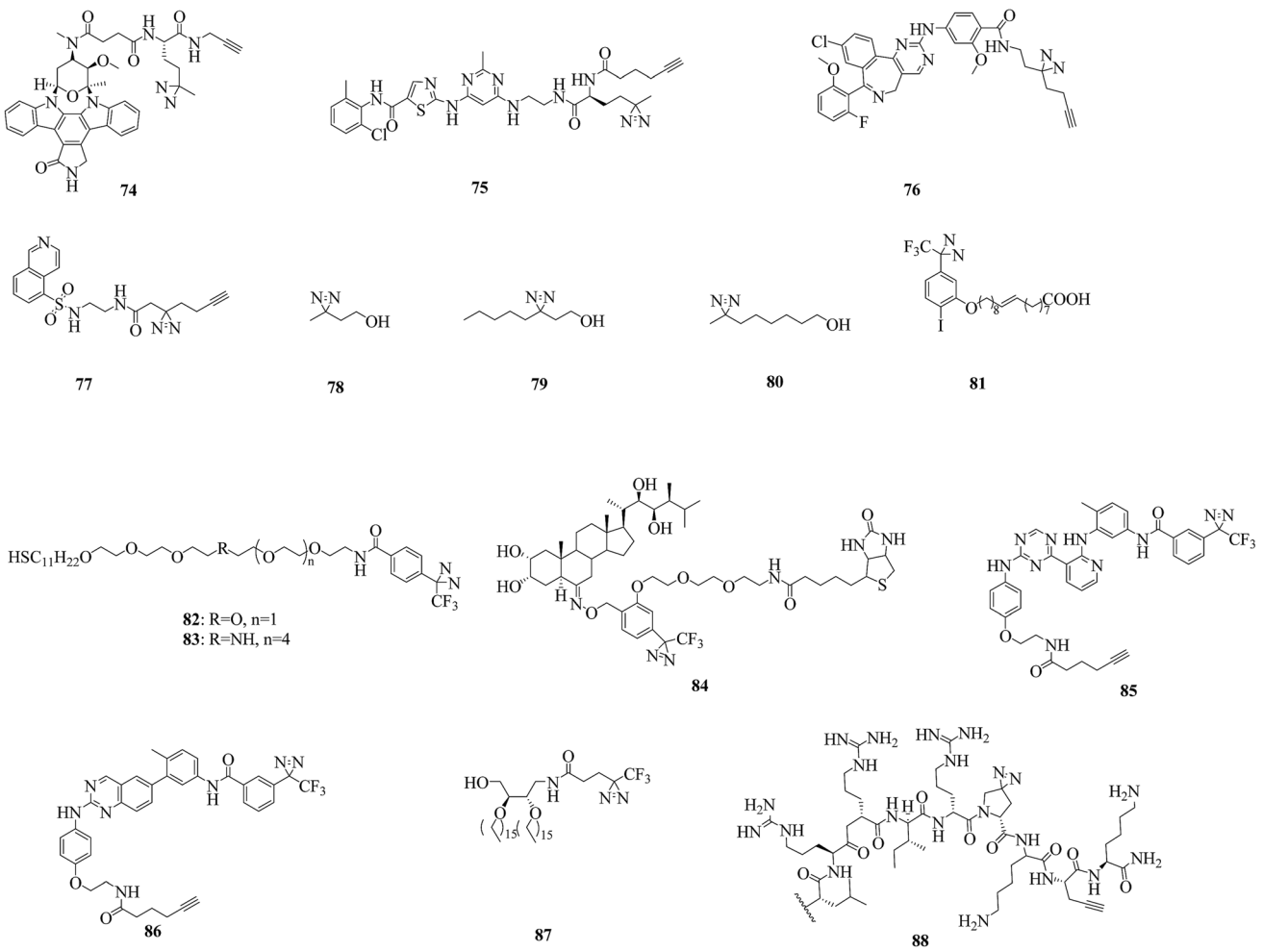

Fig. 13 Representative applications of cmPAL for studying kinases.

PKD2.[75] In addition, a leucine-rich repeat (LRR) receptor serine/threonine kinase, namely, brassinosteroid insensitive 1 (BRI1), which is localized in the plasma membrane,[167] was studied using biotin-tagged photoaffinity castasterone (BPCS, **84**, Fig. 13), which revealed that brassinosteroids bind directly to the 94 amino acids that constitute ID-LRR22 in the extracellular domain of BRI1 and defined a new binding domain for steroid hormones.[168]

Other kinases, including type II kinases,[169] diacylglycerol kinases (DGKs)[170] and a bacterial sensor kinase, namely, ParS,[80] have also been used as models to investigate the binding sites of their inhibitors or the structure of their catalytic domains. The use of two probes **85** and **86** directed to the active site (Fig. 13), which were derived from type II ATP-competitive inhibitors, in combination with stable-isotope labeling with amino acids in cell culture (SILAC) and mass spectrometry resulted in the identification of a diverse set of targets of protein kinases that were selectively enriched.[169] Photoaffinity labeling of a probe **87** (Fig. 13) demonstrated that the crosslinking efficiency depended on the length of the linker between the photocrosslinker and the diacylglycerol-like moiety in the probe: probes that contained longer linkers could access the active site and be used as substrates.[170] Similarly, a probe DYN5 (**88**, Fig. 13) that contained a diazirine-modified photo-proline in place of proline triggered a clear virulence response in *Pseudomonas aeruginosa*, which was consistent with the probes DYN4, DYN3, and DYN1, which contained an aryl azide moiety or a benzophenone moiety incorporated at the C-terminus of the sequence or in place of phenylalanine, respectively.[80]

4.2. γ-Secretase

A particularly challenging target for drug discovery is γ-secretase, which is an intramembrane aspartyl protease complex that cleaves amyloid precursor proteins (APPs) to release Aβ peptides, which probably play a causative role in the pathogenesis of Alzheimer's disease (AD). Hence, the inhibition of the processing of APPs using γ-secretase inhibitors is one of the most important strategies for the prevention and treatment of AD. Over the past several years, a number of photoprobes have been reported to provide a greater understanding of ligand-binding sites within γ-secretase.

The caprolactam-type dipeptide γ-secretase inhibitors CE (**89**, Fig. 14) and DBZ (**90**, Fig. 14) are analogues of DAPT (**91**, Fig. 14), which is a compound that exhibits excellent γ-secretase-inhibitory activity in APP-transgenic mice.[171] In order to elucidate the enzyme specificity of dipeptide γ-secretase inhibitors, Fuwa *et al.* developed a set of multifunctional molecular probes based on CE and DBZ by means of a copper(I)-mediated azide/alkyne fusion process. Despite their robust inhibitory activities against the production of Aβ, which were comparable to those of the parent compounds, two benzophenone probes with an ethylene glycol linker and phenyldiazirine groups (**92** and **93**, Fig. 14) were ineffective in photoaffinity labeling experiments, which reflected the difficulties in the "rational" design of an effective multifunctional photoprobe, even if sufficient information about the SARs of an affinity ligand moiety is provided.[172] A similar case was described by Crump *et al.*, who modified BMS-163 (Fig. 14), which is a non-selective γ-secretase inhibitor,[173] with a clickable moiety and various photoreactive groups to target γ-secretase *in vitro* and in cells. Benzophenone probes based on BMS-163 covalently labeled PS1-NTF, whereas the diazirine-containing probe 163-DZ (**94**, Fig. 14) did not, which further demonstrates that benzophenone is preferred over diazirine as a photoreactive group for labeling γ-secretase.[174]

In contrast, several highly potent acidic γ-secretase modulators (GSMs) that lowered Aβ42 levels in cellular assays with nanomolar modulatory activity were modified by Rennhack *et al.*, who introduced photoreactive diazirine moieties into the acidic GSM scaffolds according to an analysis of their SARs. Most of these retained a strong ability to lower Aβ42 levels that was comparable to the potency of the parent compound and may be potential photoreactive reagents for crosslinking the N-terminal fragment of presenilin (PSEN, the catalytic subunit of the γ-secretase complex).[175] In addition, Jumpertz *et al.* used GSM-based photoprobes such as AR80, AR243, and AR366 (**95–97**, Fig. 14) to investigate the molecular mechanism of GSMs. By using established cell-free conditions and living cells, PSEN was identified as the molecular target of potent acidic GSMs. Further studies indicated that potent acidic GSMs target PSEN to modulate the enzymatic activity of the γ-secretase complex. The inverse modulator AR366, which exhibits micromolar potency, represented an interesting tool for further investigations.[176] Furthermore, these diazirinyl probes were successfully crosslinked to PSEN, which suggested that diazirine is a viable option for targeting γ-secretase.

4.3. Methyltransferases

Methyltransferases (MTs), which constitute one of the largest classes of enzymes in nature, can catalyze the methylation processes of many biomolecules such as DNA, RNA, and metabolites. With the help of various *S*-adenosylmethionine (SAM)-dependent MTs, methyl groups are extensively introduced into these biomolecules, so that the biomolecules are structurally and functionally diversified. The metabolic product of catalysis, namely, *S*-adenosyl-L-homocysteine (SAH), can then be further catabolized to homocysteine, converted into methionine, and reincorporated into SAM.[177] Because methylation can control DNA transcription both directly *via* DNA methylation and indirectly *via* histone methylation, MTs can be mainly classified into two types, namely, DNA methyltransferases (DNMTs) and histone methyltransferases (HMTs), on the basis of the substrate of methylation in vertebrates. Given their important role in epigenetic control, lipid biosynthesis, protein repair, hormone inactivation, and tissue differentiation[178] and the fact that a large fraction of the human MT family remains poorly understood, significant efforts have been made to identify and characterize MTs and their inhibitors in native biological systems over the past decade.

In a related study, He *et al.* expressed and purified *E. coli* DNA adenine methyltransferase (EcoDam), which is an enzyme that methylates the N-6 position of adenine in GATC sequences,

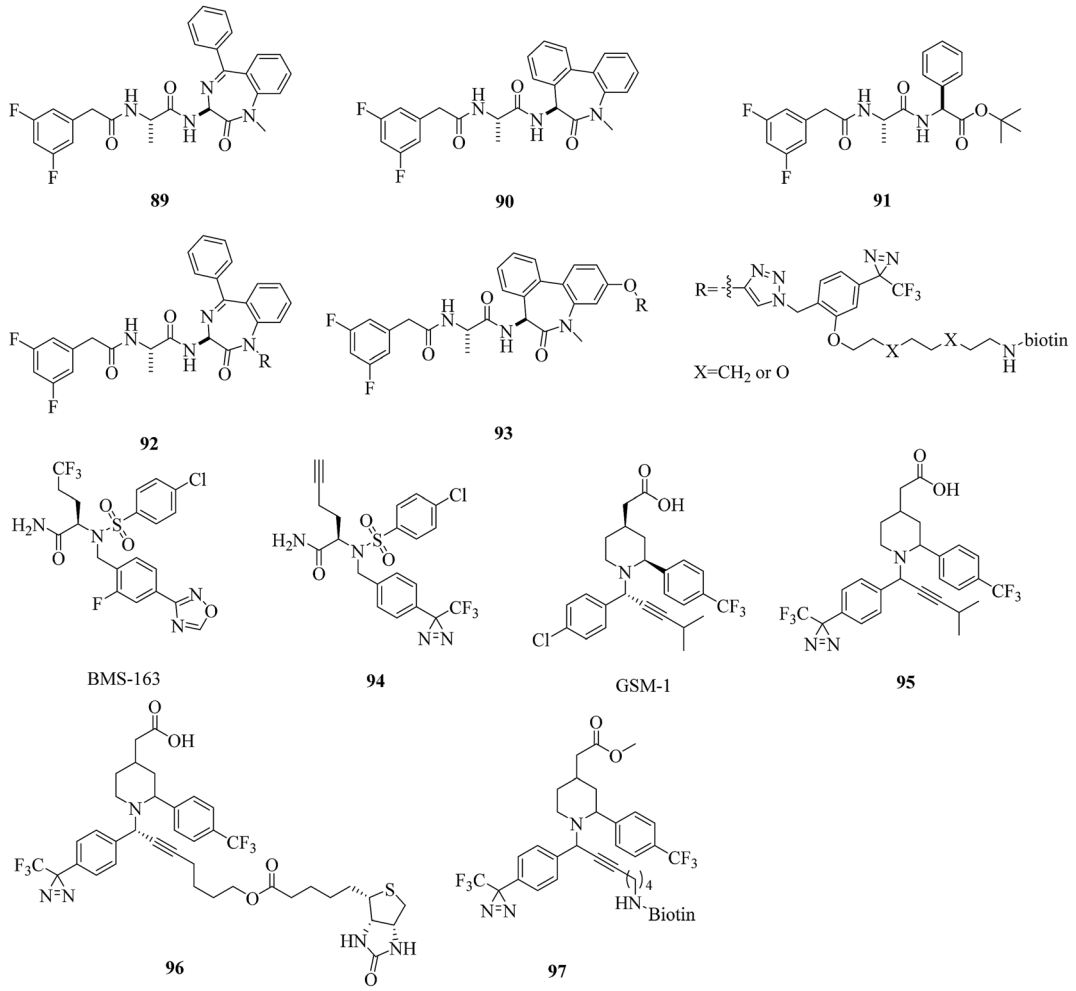

Fig. 14 Representative applications of cmPAL for studying γ-secretase.

to investigate its photocrosslinking to various diazirinyl DNA probes such as the cytosine- and guanine-based probes **20** and **21** (illustrated in Fig. 7). After crosslinking with EcoDam, good to excellent yields of the resulting DNA probes bearing a diazirine unit were observed, which would provide valuable information about how EcoDam binds to the corresponding DNA.[93] Similarly, in order to carry out the selective photoinduced isolation of MTs, Dalhoff *et al.* synthesized a series of SAH-based capture compounds that carried a TPD moiety or an azide group (**98** and **99**, Fig. 15). When tested using purified MTs, these SAH-based capture compounds exhibited a certain applicability in the determination of the dissociation constant K_D of MT-cofactor complexes and the isolation of SAH-binding enzymes from an *E. coli* cell lysate.[179] In another case, Horning *et al.* used a suite of SAH photoaffinity probes bearing different photoexcitable groups, as well as chemical proteomics experiments, to specifically profile and enrich MTs from human cancer cell lysates. In addition to enriching MT-associated proteins, these SAH probes were used to successfully discover a covalent inhibitor of nicotinamide *N*-methyltransferase (NNMT), which is an enzyme implicated in cancer and metabolic disorders. Furthermore, study results revealed that SAH-based diazirinyl probes (**100** and **101**, Fig. 15) were capable of enriching a substantial fraction of human MTs, and the aliphatic diazirine group exhibited the broadest and most specific coverage of MTs from cancer cell proteomes among different photoreactive groups.[180]

Isoprenylcysteine carboxyl methyltransferases (Icmts) are not only a class of SAM-dependent enzymes that catalyze the carboxymethylation process but are also localized in the membrane of the endoplasmic reticulum. Methylation catalyzed by Icmts can lead to the generation of **a**-factor, which is a naturally occurring farnesylated peptide found in yeast. In order to investigate methyltransferases, Vervacke *et al.* incorporated a diazirine-containing isoprenoid unit into a biotinylated and fluorescently labeled **a**-factor peptide analogue (**102**, Fig. 15). Then the probe was evaluated using a recombinant Icmt (Ste14p) that incorporated both a His_{10} tag for purification and a triply repeated *myc* tag to facilitate detection by immunoblotting analysis (His-Ste14p). The greater yield of photocrosslinked His-Ste14p, coupled with the ease of analysis achieved with the probe, suggested that this new class of isoprenoid analogues should be more widely used in studies of enzymes that act on terpene-derived molecules.[181]

DOT1L is not only the sole protein methyltransferase that methylates histone H3 on lysine 79 (H3K79) but is also

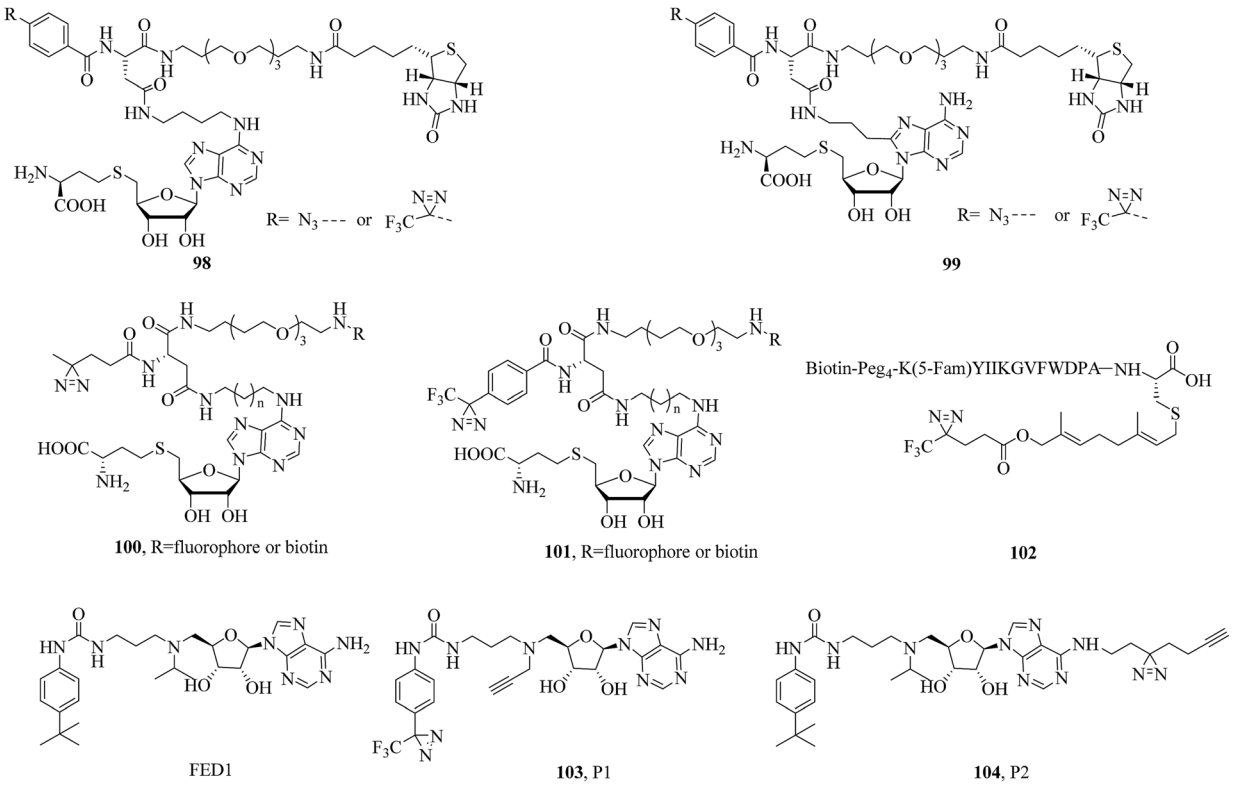

Fig. 15 Representative applications of cmPAL for studying methyltransferases.

a promising target for anticancer drugs. Yao *et al.* designed and synthesized two clickable AfBPs, namely, P1 and P2 (**103** and **104**, Fig. 15), which were based on a scaffold of FED1 (Fig. 15), which is a potent DOT1L inhibitor and structural mimic of SAM, to study potential cellular off-targets of FED1 in native cellular environments. In combination with quantitative LC-MS/MS, as well as chemical proteomics approaches, NOP2 (a putative ribosomal RNA methyltransferase) was confirmed to be probably a genuine off-target of FED1. Live-cell imaging experiments showed that most probes were not able to reach the cell nucleus, where functional DOT1L resides in mammalian cells, which provided a plausible explanation of the poor cellular activity of FED1.[182]

4.4. Metalloproteinases

Metalloproteinases (MPs), of which the catalytic mechanism involves a metal, are the most diverse of the four main types of protease, and more than 50 families have been classified to date. There are two subgroups of MPs, namely, metalloexopeptidases and metalloendopeptidases. Well-known metalloendopeptidases include matrix MPs (MMPs) and a disintegrin and MPs (ADAMs), both of which are catalytically active Zn^{2+}-dependent proteins and have important physiological functions. MMPs play a central role in the degradation of extracellular matrix proteins (gelatin, elastin, and collagen).[183–185] ADAMs are membrane-anchored MPs that contain both a cellular adhesion domain and an MMP domain and are involved in cell migration, muscle development, and fertilization, and so on.[186,187] The biological importance of these two classes of enzymes has made the development of chemical tools for their study an important and active field of research in recent years.

In a related study, Chan *et al.* reported a diazirinyl probe (**105**, Fig. 16) that carried a similar succinyl hydroxamate moiety as the zinc-binding group (ZBG) and a Cy3 dye as the substrate recognition unit for identifying catalytic sites of MPs. After a PAL experiment, the probe successfully targeted MMP-9 enzyme from a crude yeast extract with high sensitivity and selectivity. Furthermore, the extent of labeling was found to be dependent on the catalytic activity of the enzyme. Given the significant roles that many MPs play in a variety of diseases, this strategy may serve as a useful tool for potential therapeutics.[188] In another case, Leeuwenburgh *et al.* synthesized a peptide hydroxamate analogue (**106**, Fig. 16) that featured both a biotin moiety and a TPD moiety *via* a solid-phase synthesis strategy. Upon incubation of purified recombinant ADAM-10 and subsequent photoaffinity labeling, the MP was covalently and irreversibly modified, which makes probe **106** a promising candidate for profiling ADAMs or MMPs.[189] In addition, Geurink *et al.* modified a succinyl hydroxamate moiety by placing a TPD group at the P1′-position to make a more effective probe with which active MPs can be profiled and visualised. Evaluation using purified recombinant ADAM-17 revealed that positioning the photoactivatable group at the P1′-position, as in **107** (Fig. 16), makes a photoactivatable activity-based probe for MMP/ADAM comparatively more potent than previously. It was also demonstrated that the photoactivatable group should be directed towards the S1′ pocket, rather than the S2′ pocket.[190]

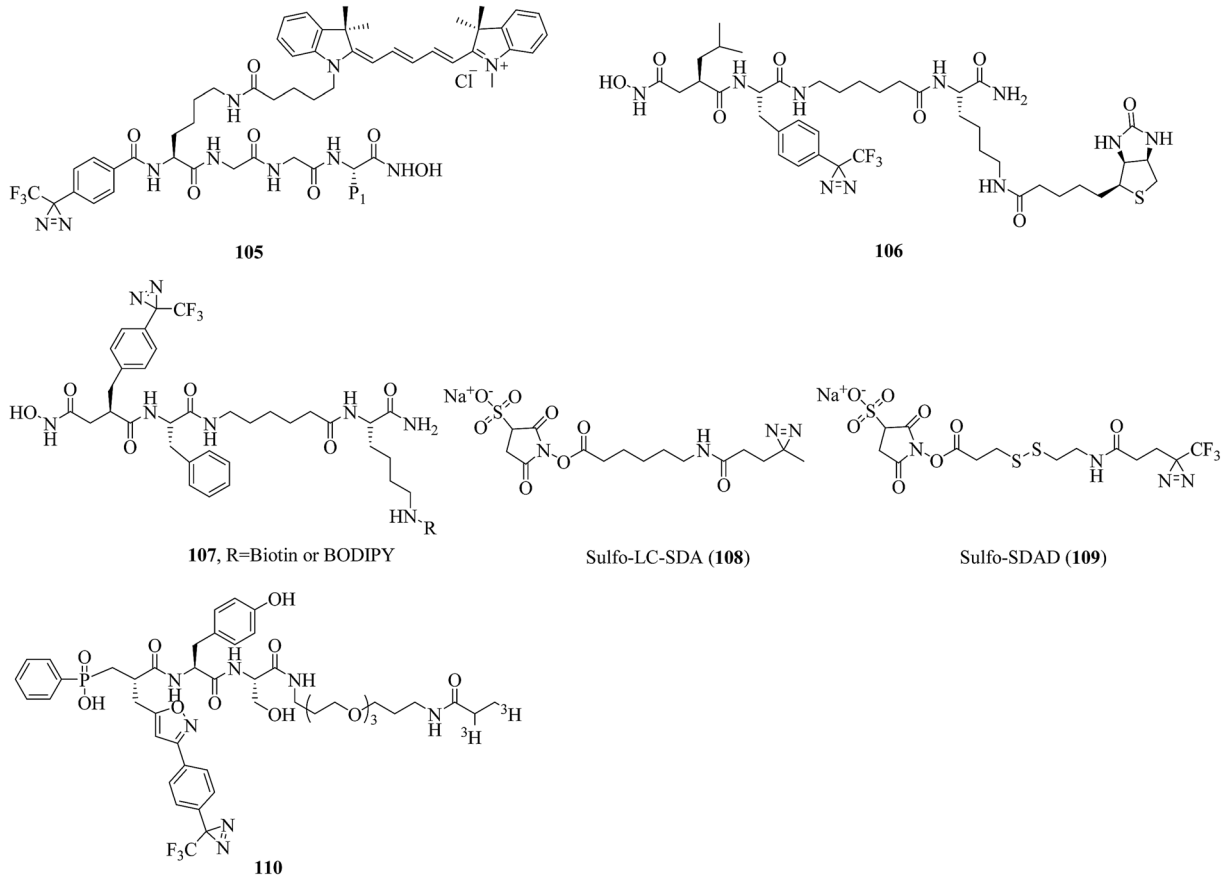

Fig. 16 Representative applications of cmPAL for studying metalloproteases.

Lozito *et al.* reported two heterobifunctional crosslinkers, namely, sulfo-LC-SDA (**108**, Fig. 16) and sulfo-SDAD (**109**, Fig. 16), which contained negatively charged sulfate groups to improve their solubility and diazirine units to identify specific interactions between TIMPs (tissue inhibitors of MPs) and MMPs contributed by MSCs (mesenchymal stem cells) and ECs (endothelial cells) in biological environments. It was demonstrated that MSCs inhibit both endogenous and exogenous MMPs *via* secreted TIMPs. Under control conditions, TIMP-2 and TIMP-1 protect the niche from MMP-2 and MMP-9, respectively. An investigation of the interactions between MMP-2 and TIMPs showed that TIMP-2 was the primary inhibitor of endogenous MMP-2. Nevertheless, under pathological stress MSCs act as a critical perivascular source of vessel-stabilizing TIMPs that are capable of protecting the vascular environment from disruption by proteases.[191] In another example, Nury *et al.* reported a diazirinyl photoprobe (**110**, Fig. 16), which was based on a scaffold of a potent broad-spectrum phosphinic peptide inhibitor of MMPs, for detecting active forms of MMPs from biological fluids or tissue extracts. In the characterization of seven catalytic domains of human MMPs, the probe displayed high sensitivity in the detection of these MMPs. Furthermore, the probe permitted simultaneous detection with low background labeling in a complex proteome supplemented with four recombinant MMPs (MMP-2, -9, -12 and -13).[192]

4.5. Histone deacetylase

Histone deacetylases (HDACs) are hydrolases that catalyze the removal of acetyl groups from the ε-amino groups of lysine residues in histones or other cellular proteins, which allows the histones to wrap DNA more tightly. They thus play important roles in regulating various physiological and pathological processes.[193–196] There are three classical HDACs, namely, Classes I, II, and IV, of which the activity is zinc-dependent. In addition, Class III consists of NAD^+-dependent protein deacetylases known as sirtuins 1–7 (Sirt1–7).[197] Many sophisticated studies of HDACs or HDAC inhibitors have been reported in the past three years.

A related study was described by Hentschel *et al.*, who developed the first photoreactive psammaplin A (**111**, Fig. 17), which was as potent an HDAC inhibitor (IC_{50} = 35 nM) as the parent compound psammaplin A (Fig. 17). Its very similar cytotoxicity profile to that of psammaplin A makes compound **111** a candidate for cmPAL, which may assist in the identification of new targets of psammaplin A and a better understanding of the mode of action with zinc-dependent HDACs.[198] For the single-step detection and proteomic profiling of HDACs, Xie *et al.* developed a novel fluorescent probe (**112**, Fig. 17) by combining a Kac (*N*-acetyllysine) recognition unit, an O-NBD (nitrobenzoxadiazole) fluorophore and a minimalist photocrosslinker. It was a breakthrough finding that epigenetic

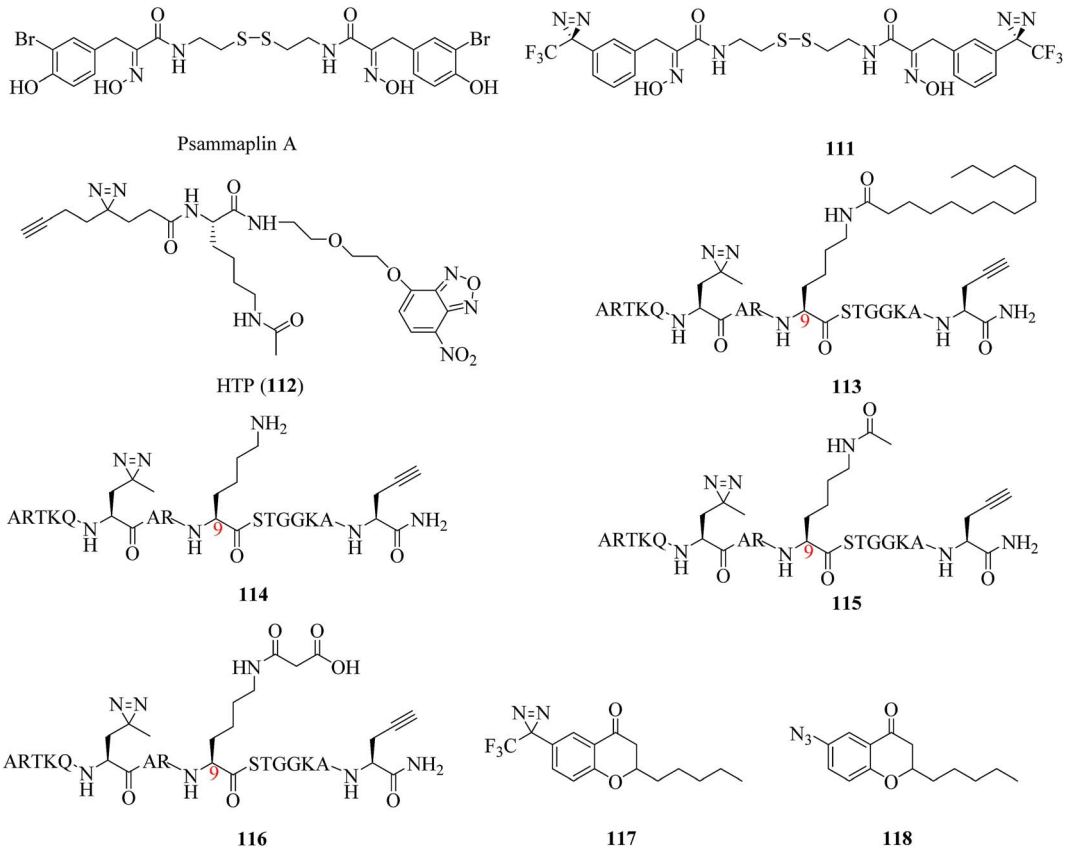

Fig. 17 Representative applications of cmPAL for studying histone deacetylases.

readers and erasers can be readily identified and differentiated by using a single probe in combination with an in-gel fluorescence scanning technique and pull-down assays in comparison with traditional AfBPs. Furthermore, it was demonstrated that the probe can not only detect enzymatic activity but also directly identify protein targets in the native cellular environment. Such a strategy provides a robust tool for functional analysis of HDACs and facilitates future drug discovery in epigenetics.[199]

In another study, Liu *et al.* designed and synthesized a diazirinyl photoprobe (**113**, Fig. 17), which was based on a scaffold of a Lys9-myristoylated histone H3 peptide (H3K9Myr), and a K9-unmodified control probe (**114**, Fig. 17), which were coupled with a series of chemical biology approaches such as cmPAL, SDS-PAGE, and in-gel fluorescence scanning to examine human sirtuins as fatty acid deacylases *in vitro* and in cells. Sirt6, which is an enzyme that catalyzes the removal of the myristoyl group from the H3K9Myr peptide *in vitro*, was selectively captured by probe **113** but not by the unmodified control probe **114**, which suggested that probe **113** can be used to examine the interactions between *N*-myristoylated lysine and its erasers. In the same way, another two classes of sirtuins, namely, Sirt2 and Sirt3, were also successfully labeled, which revealed their potential to recognize the myristoylation of lysine. As it is preferentially labeled by probe **113** in complex protein mixtures, Sirt2 exhibits stronger interactions with H3K9Myr than other tested sirtuins.[200] In addition, Yang *et al.* developed two AfBPs, namely, **115** and **116** (Fig. 17), which were based on a histone H3 peptide in which the residue Lys9 was acetylated and malonylated, respectively, as well as the same control probe **114** to identify 'erasers' of histone lysine acylation. When reacted with recombinant human Sirt3 and Sirt5, probes **115** and **116** selectively labeled Sirt3 and Sirt5, respectively, whereas the control probe **114** failed to capture either of these enzymes, which suggested that probes **115** and **116** are ideal photoreactive reagents for the identification of their corresponding 'erasers'. Furthermore, these two probes can specifically identify and enrich endogenous Sirt3 and Sirt5, respectively, from complex HeLa S3 lysates, which demonstrated that diazirine-based AfBPs are also useful tools for trapping erasers of histone lysine acylation from a complex biological environment.[201] In brief, this strategy enables applications for both examining interactions between other PTMs and their erasers and revealing unknown cellular mechanisms controlled by sirtuins.

Similarly, according to an analysis of the SAR, a potent Sirt2 inhibitor was described by Seifert *et al.*, who used two chroman-4-one-based AfBPs, namely, **117** and **118** (Fig. 17), which carried a diazirine moiety and an azide group, respectively, to identify the binding site of isoform-selective Sirt2 inhibitors. Of these probes, the diazirinyl probe **117**, which displayed higher activity in the inhibition of Sirt2 ($IC_{50} = 8.2$ μM) than probe **118**, which carried an azide group, was examined using recombinant Sirt2. The cmPAL experiments with the enzyme followed by tryptic digestion and LC-MS/MS analysis located the binding site of

probe **117** in the tryptic peptide I175-K210, which includes the binding site of chroman-4-one-based Sirt2 inhibitors. Furthermore, the irradiation times (3×10 s) in the cmPAL experiments were reduced using a high-power LED to avoid undesirable labeling of Sirt2.[202]

4.6. Other enzymes

DNA polymerase β, which is an enzyme that interacts significantly with the sugar–phosphate backbone of DNA, is predominantly involved in DNA replication and carries out processive replication of chromosomal DNA during cell division in eukaryotes.[203] A related study was reported by Yamaguchi *et al.*, who incorporated some phosphoramidite derivatives of **119** (Fig. 18) into oligonucleotides *via* solid-phase synthesis to label mammalian DNA polymerase. Upon irradiation with near-UV light, the photolabile oligonucleotides were successfully crosslinked to recombinant rat DNA polymerase β, which suggested that they may be useful for extending the study of DNA–protein interactions.[204] Similarly, Liebmann *et al.* reported the labeling of DNA polymerase β *via* the attachment of a light-sensitive TPD moiety to the C-4′ position of 2′-deoxyribose. Modification of the pentose moiety in the incorporated thymidine **120** (Fig. 18) enabled an investigation of the interactions in the minor groove of the helix. The new photoactive building block based on TPD selectively labeled DNA polymerase β even in the presence of BSA, which revealed that it would enable several applications in investigations of DNA backbone interactions in the minor groove.[205]

ATPases are enzymes that catalyze the decomposition of ATP into ADP and a free phosphate ion. There are different types of ATPase, which differ in function, structure (F-, V- and A-ATPases contain rotary motors) and the types of ion that they transport (Na/K-ATPases transport sodium and potassium ions across the plasma membrane).[206–208] In a related study, Blanton *et al.* synthesized a radiolabeled diazirine probe [^{125}I]TID (**121**, Fig. 19) and a phosphatidylcholine analogue [^{125}I]TIDPC/16 (**122**, Fig. 19) to identify a lipid–protein interface, namely, the lipid-exposed transmembrane segments and transmembrane structural transitions of *Torpedo* Na/K-ATPase. A photolabeling experiment using probe **122** and Na/K-ATPase in combination with an analysis of the amino-terminal sequence of proteolytic fragments showed that the primary binding sites were localized in the hydrophobic segments M1, M3, M9, and M10, which constitute the major part of the lipid–protein interface in the α-subunit of Na/K-ATPase. Studies of the conformational sensitivity of probe **121** suggest that this radiolabeled diazirine probe would be a useful tool for structural characterization of the cation translocation pathway and conformationally dependent changes in the pathway.[209] In addition, in order to study the binding sites of 21-deoxyconcanolide A and bafilomycin A_1, which are two specific inhibitors of V-type ATPase (a proton translocation machine and pH regulator in almost all eukaryotic cells), Bender *et al.* incorporated a radiolabeled diazirine probe (**123**, Fig. 19) into two AfBPs (**124** and **125**, Fig. 19), which were based on a scaffold of 21-deoxyconcanolide A and bafilomycin A_1, respectively. Both these AfBPs exhibited high inhibitory activity, which thus makes them ideal candidates for the further identification of the precise binding site of these potent V-ATPase inhibitors.[210]

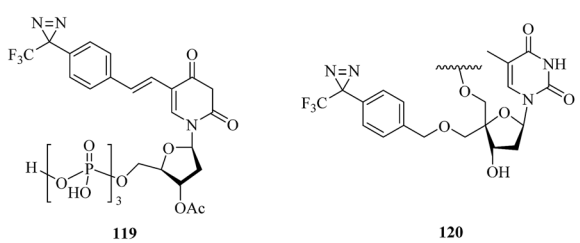

Fig. 18 Representative applications of cmPAL for studying DNA polymerase.

Another well-known enzyme is protein tyrosine phosphatase 1B (PTP1B), which belongs to the protein tyrosine phosphatase (PTP) family and is involved in downregulating the insulin receptor and can serve as a target of drugs for the treatment of type II diabetes.[211] To better understand the mode of action of PTP1B inhibitors, a cell-based assay for directly measuring the enzyme occupancy of PTP1B by inhibitors using cmPAL was developed by Skorey *et al.*, who synthesized two diazirine-based AfBPs, namely, **126** and **127** (Fig. 20), of which the most potent photoprobe exhibited an IC_{50} value of 0.2 nM for PTP1B. The photoaffinity assay of enzyme occupancy was successfully performed with both purified recombinant FLAG-tagged PTP1B and endogenous PTP1B in intact and lysed HepG2 cells, which indicated that these two compounds are powerful tools for research into PTP1B inhibitors.[212]

The removal of an N-terminal methionine residue from nascent polypeptides is dependent upon a unique class of proteases typified by the dinuclear metalloenzyme methionine aminopeptidase (MetAP) from *Escherichia coli*. Although the identification of human MetAP as the target of putative anticancer drugs reiterates the importance of this family of enzymes,[213] the physiological function of MetAP1 (type 1 MetAP), however, has remained elusive. In a related study, Qiu *et al.* modified the potent MetAP1 inhibitor L134 ($IC_{50} = 0.049$ nM) with a TPD moiety and a photostable azido-acetyl group to prepare two trimodular photoaffinity probes (**128** and **129**, Fig. 21), which retained their inhibitory activity toward EcMetAP1, with nanomolar IC_{50} values. Then these probes were evaluated using purified recombinant EcMetAP1 and a crude cell lysate containing overexpressed MetAP1. Both of them were capable of labeling a 30 kDa polypeptide, which corresponded to the predicted molecular weight of EcMetAP1. In the presence of the competitive inhibitor L288, the signal intensities for the 30 kDa species were obviously reduced, whereas the signals for the 60 and 28 kDa species displayed no sensitivity to L288, which suggested that the 30 kDa polypeptide labeled by probe **128** was the native MetAP1. In addition, probe **129** was more effective than probe **128** despite the similarity in their IC_{50} values, which demonstrated that the length of the linker was a contributing factor. The trimodular probe **129** provided much more desirable flexibility for a prototype scaffold, which also allows improvements for different applications.[214]

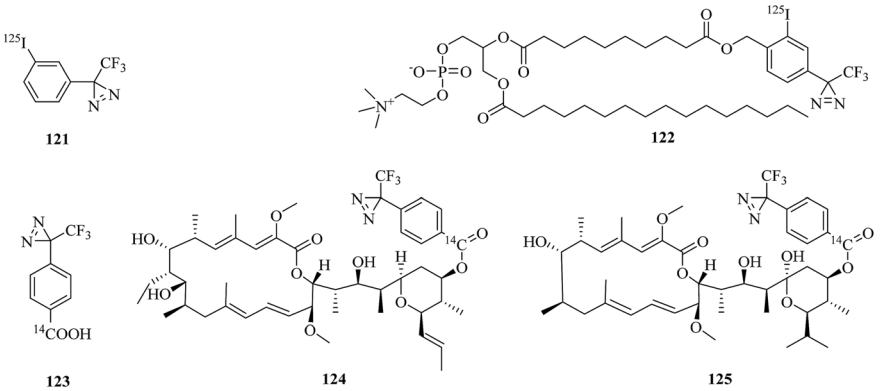

Fig. 19 Representative applications of cmPAL for studying ATPases.

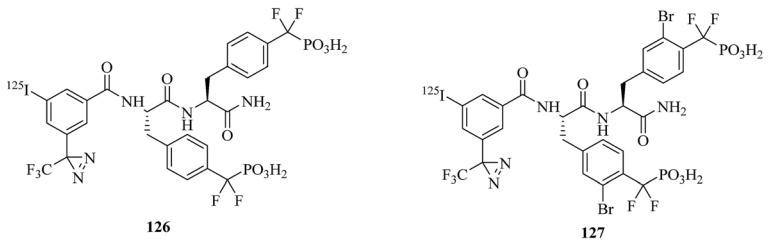

Fig. 20 Representative applications of cmPAL for studying protein tyrosine phosphatase 1B.

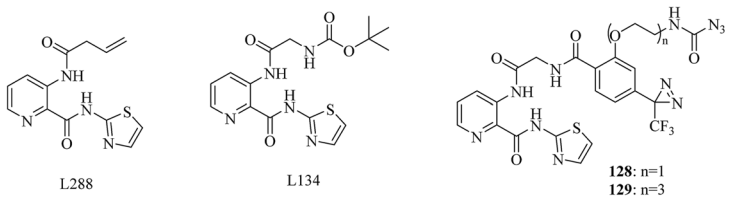

Fig. 21 Representative applications of cmPAL for studying methionine aminopeptidase.

Etoposide (Fig. 22) is a widely used anticancer drug that targets topoisomerase II, which is an essential nuclear enzyme, with an unknown mode of binding. In order to identify the sites of binding between etoposide and topoisomerase II, Chee *et al.* developed a diazirinyl photoprobe (**130**, Fig. 22), which was based on a scaffold of etoposide. A set of characterizations of its photoreactivity and biological activities indicated that this photoaffinity label binds topoisomerase II with a similar affinity. It is worth mentioning that this diazirinyl photoprobe should be a promising tool for identifying the binding sites of etoposide in topoisomerase II.[215]

Sialidases, which are also known as neuraminidases, are enzymes that catalyze the hydrolysis of terminal sialic acid residues in oligosaccharides, glycoproteins, and glycolipids.[216] In order to improve the utility of the diazirine-based sialic acid analogue SiaDAz (**131**, Fig. 23), McCombs *et al.* screened a panel of sialidases to find one that would cleave natural sialic acids but remain inactive toward SiaDAz. The results of the study demonstrated that the crosslinking of SiaDAz-modified glycoconjugates can be enhanced by pre-treating cells with STNA (*Salmonella typhimurium* neuraminidase), which is a commercially available sialidase that removes the natural sialic acid Neu5Ac, but not SiaDAz. This strategy can be applied generally to sialic acid-mediated interactions and facilitate the identification of binding partners of sialic acid.[121] In another study, Rodriguez *et al.* modified the N-acyl side chain of GlcNAc (**132**, Fig. 23) with an alkyldiazirine to prepare a photoprobe GlcNDAz (**133**, Fig. 23) and used the probe to examine the activity of recombinant human O-GlcNAc hydrolase (OGA), which is an enzyme that removes O-GlcNAc groups from serine and threonine residues in intracellular glycoproteins. Recombinant human OGA is unable to hydrolyze an O-GlcNDAz mimic or to remove an O-GlcNDAz group from a peptide, which provides new insights into the recognition of substrates by OGA, which is an important drug target.[217]

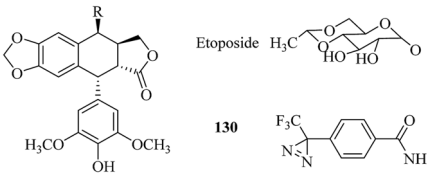

Fig. 22 Structures of 4′-demethyl-4*b*-podophyllotoxin derivatives.

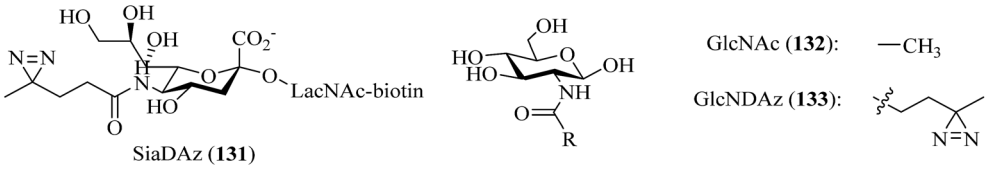

Fig. 23 Representative applications of cmPAL for studying sialidases.

In order to acquire a better understanding of the pharmacological effects of LW6 (Fig. 24) and its relation to HIF-1α and malate dehydrogenase 2 (MDH2), Naik *et al.* synthesized a probe as an LW6 mimic (**134**, Fig. 24), which contained a photoactive diazirine group. Both *in vitro* binding between the probe and recombinant human MDH2 *via* cmPAL and competitive inhibition of MDH2 activity with NADH, as in the case of LW6, were successfully confirmed, which suggested that the probe should provide a more comprehensive understanding of LW6 and MDH2.[218] Similarly, Bongo *et al.* described the general use of a diazirinyl probe (**135**, Fig. 24) as a photoreactive mimic of α-amino acids, which can be cleaved upon treatment with a mild base to facilitate the retrieval of biotin-tagged proteins, as well as peptides, from avidin matrices. Upon irradiation with UV light, this diazirinyl probe specifically cross-linked glutamyl endopeptidase, L-glutamate dehydrogenase, glutamate oxaloacetate transaminase and L-glutamine synthetase, which are all enzymes that exhibit high affinity toward acidic α-amino acids. Its simple synthesis, coupled with its multifunctional nature, suggested that the probe would be a versatile photoreactive building block.[219]

CmPAL using a diazirinyl photoprobe to covalently bind its target in response to activation by light has become a frequently used tool for studying potential cellular targets of enzymes or their inhibitors and identifying the location and structure of binding sites. Recent efforts have mainly focused on cmPAL using a large panel of photoaffinity probes, as well as mass spectrometry-based chemical profiling methods, to identify binding sites and reveal unknown cellular mechanisms controlled by enzymes or corresponding inhibitors. Here, we have discussed different applications of cmPAL for classes of enzymes, including kinases, γ-secretase, methyltransferases, metalloproteinases, histone deacetylases, and so on. Although in some cases a benzophenone was the logical choice of label given the structure of the pharmacophore, it might be expected that diazirines will become the dominant photoreactive group and even develop into a versatile platform for labeling enzymes in the future as a development of synthetic methods involving the direct introduction of a minimalist crosslinker bearing an alkyldiazirine moiety and a terminal alkyne or TPD functionality into probe scaffolds.

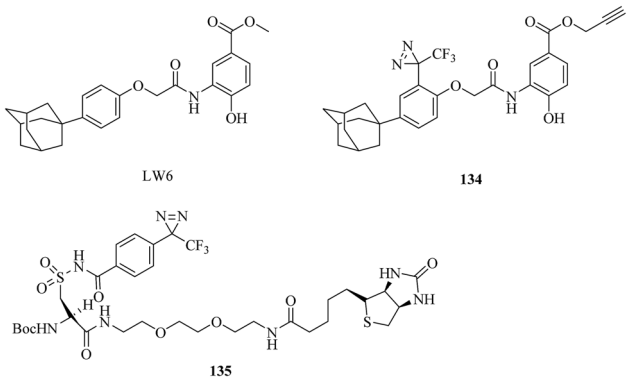

Fig. 24 Structures of photoreactive acidic α-amino acid analogues.

5. Conclusions and outlook

As discussed in this review, the applications of cmPAL have established its uniquely important place in the identification of targets or binding sites in recent years. In particular, as precursors of carbenes, diazirines, which have been shown to be the most promising photoreactive reagents used for cmPAL, have enabled different types of sophisticated derivatization of diazirinyl probes according to the type of the parent ligand molecule. Supported by the development of analytical techniques, much more effort has been devoted to revealing unknown cellular mechanisms and drug–target binding sites controlled by various enzymes, especially inactive enzymes and corresponding inhibitors, by using a large panel of diazirine-based biological probes. Furthermore, the use of several probes for different classes of enzymes with different photoaffinity groups located in different regions may be necessary to provide a more comprehensive tool. In spite of the successful examples reported in this review, a continuing challenge in cmPAL involves the rational design of photoaffinity probes, which should retain the potency and specificity of the parent compounds, with less non-specific photolabeling and better accuracy in the proteome-wide identification of targets *via* MS analysis. Given these limitations, this is understandable, and clearly an urgent need still exists for the chemical biology community to develop more rational cmPAL-based probes for uncharacterized drug candidates and enzyme families relevant to various human diseases in particular. In addition, drugs and inhibitors need not be the only components of the proteome examined by cmPAL. Future research may provide insights into the development of cmPAL for investigating receptors and structural proteins.

Conflicts of interest

There are no conflicts to declare.

Acknowledgements

We wish to thank the financial support from the Key Technologies R&D Program (2014BAD23B01), the National Natural Science Foundation of China (21372052), and the Research Project of the Chinese Ministry of Education (213033A, 20135201110005).

References

1 A. Singh, E. R. Thornton and F. H. Westheimer, *J. Biol. Chem.*, 1962, **237**, 3006–3008.
2 M. Hashimoto and Y. Hatanaka, *Eur. J. Org. Chem.*, 2008, 2513–2523.
3 Y. Tanaka, M. R. Bond and J. J. Kohler, *Mol. BioSyst.*, 2008, **4**, 473–480.
4 E. Smith and I. Collins, *Future Med. Chem.*, 2015, **7**, 159–183.
5 K. Sakurai, S. Ozawa and T. Yamaguchi, *Bioorg. Med. Chem.*, 2015, **23**, 5319–5325.
6 J. Park, M. Koh, J. Y. Koo, S. Lee and S. B. Park, *ACS Chem. Biol.*, 2016, **11**, 44–52.
7 Y. Tian, M. P. Jacinto, Y. Zeng, Z. Yu, J. Qu, W. R. Liu and Q. Lin, *J. Am. Chem. Soc.*, 2017, **139**, 6078–6081.
8 A. Herner, J. Marjanovic, T. M. Lewandowski, V. Marin, M. Patterson, L. Miesbauer, D. Ready, J. Williams, A. Vasudevan and Q. Lin, *J. Am. Chem. Soc.*, 2016, **138**, 14609–14615.
9 O. A. Battenberg, M. B. Nodwell and S. A. Sieber, *J. Org. Chem.*, 2011, **76**, 6075–6087.
10 J. Sumranjit and S. J. Chung, *Molecules*, 2013, **18**, 10425–10451.
11 F. Ford, T. Yuzawa, M. S. Platz, S. Matzinger and M. Fülscher, *J. Am. Chem. Soc.*, 1998, **120**, 4430–4438.
12 A. Blencowe and W. Hayes, *Soft Matter*, 2005, **1**, 178–205.
13 S. A. Fleming, *Tetrahedron*, 1995, **51**, 12479–12520.
14 R. A. G. Smith and J. R. Knowles, *J. Am. Chem. Soc.*, 1973, **95**, 5072–5073.
15 J. Das, *Chem. Rev.*, 2011, **111**, 4405–4417.
16 E. Smith and I. Collins, *Future Med. Chem.*, 2015, **72**, 159–183.
17 Y. Xia and L. Peng, *Chem. Rev.*, 2013, **113**, 7880–7929.
18 M. Hashimoto and Y. Hatanaka, *Eur. J. Org. Chem.*, 2008, 2513–2523.
19 L. Dubinsky, B. P. Krom and M. M. Meijler, *Bioorg. Med. Chem.*, 2012, **20**, 554–570.
20 S. Pan, H. Zhang, C. Wang, S. C. L. Yao and S. Q. Yao, *Nat. Prod. Rep.*, 2016, **33**, 612–620.
21 M. R. Aronoff, B. Gold and R. T. Raines, *Org. Lett.*, 2016, **18**, 1538–1541.
22 M. E. Meyer, E. M. Ferreira and B. M. Stoltz, *Chem. Commun.*, 2006, 1316–1318.
23 K. A. Mix, M. R. Aronoff and R. T. Raines, *ACS Chem. Biol.*, 2016, **11**, 3233–3244.
24 H. Bayley and J. R. Knowles, *Methods Enzymol.*, 1977, **46**, 69–114.
25 V. Chowdhry and F. H. Westheimer, *Annu. Rev. Biochem.*, 1979, **48**, 293–325.
26 L. Wolff, *Justus Liebigs Ann. Chem.*, 1902, **325**, 129–195.
27 W. Kirmse, *Eur. J. Org. Chem.*, 2002, 2193–2256.
28 V. Chowdhry, R. Vaughan and F. H. Westheimer, *Proc. Natl. Acad. Sci. U. S. A.*, 1976, **73**, 1406–1408.
29 L. Peng, M. L. Alcaraz, P. Klotz, F. Kotzyba-Hibert and M. Goeldner, *FEBS Lett.*, 1994, **346**, 127–131.
30 M. L. Alcaraz, L. Peng, P. Klotz and M. Goeldner, *J. Org. Chem.*, 1996, **61**, 192–201.
31 C. A. Converse and F. F. Richards, *Biochemistry*, 1969, **8**, 4431–4436.
32 C. M. Gupta, C. E. Costello and H. G. Khorana, *Proc. Natl. Acad. Sci. U. S. A.*, 1979, **76**, 3139–3143.
33 T. A. Kale and M. D. Distefano, *Org. Lett.*, 2003, **5**, 609–612.
34 T. Curtius, *Ber. Dtsch. Chem. Ges.*, 1890, **23**, 3023–3033.
35 T. Curtius, *J. Prakt. Chem.*, 1894, **50**, 275–294.
36 E. L. Myers and R. T. Raines, *Angew. Chem., Int. Ed. Engl.*, 2009, **48**, 2359–2363.
37 R. J. Baumgarten, *J. Org. Chem.*, 1967, **32**, 484–485.
38 H. H. Chou and R. T. Raines, *J. Am. Chem. Soc.*, 2013, **135**, 14936–14939.
39 S. R. Paulsen, *Angew. Chem., Int. Ed. Engl.*, 1960, **72**, 781–782.
40 E. Schmitz and R. Ohme, *Angew. Chem., Int. Ed. Engl.*, 1961, **73**, 220–221.
41 L. Pierce and V. Dobyns, *J. Am. Chem. Soc.*, 1962, **84**, 2651–2652.
42 E. Schmitz, R. Ohme and R. D. Schmidt, *Chem. Ber.*, 1962, **95**, 2714–2717.
43 J. Brunner, H. Senn and F. M. Richards, *J. Biol. Chem.*, 1980, **255**, 3313–3318.
44 R. Bonneau and M. T. H. Liu, *J. Am. Chem. Soc.*, 1996, **118**, 7229–7230.
45 T. Akasaka, M. T. H. Liu, Y. Niino, Y. Maeda, T. Wakahara, M. Okamura, K. Kobayashi and S. Nagase, *J. Am. Chem. Soc.*, 2000, **122**, 7134–7135.
46 T. Wakahara, Y. Niino, T. Kato, Y. Maeda, T. Akasaka, M. T. H. Liu, K. Kobayashi and S. Nagase, *J. Am. Chem. Soc.*, 2002, **124**, 9465–9468.
47 P. P. Geurink, L. M. Prely, G. A. van der Marel, R. Bischoff and H. S. Overkleeft, *Top. Curr. Chem.*, 2012, **324**, 85–114.
48 G. W. Preston and A. J. Wilson, *Chem. Soc. Rev.*, 2013, **42**, 3289–3301.
49 M. Platz, A. S. Admasu, S. Kwiatkowski, P. J. Cracker, N. Imai and D. S. Watt, *Bioconjugate Chem.*, 1991, **2**, 337–341.
50 L. Wang, Y. Murai, T. Yoshida, A. Ishida, K. Masuda, Y. Sakihama, Y. Hashidoko, Y. Hatanaka and M. Hashimoto, *Org. Lett.*, 2015, **17**, 616–619.
51 A. B. Kumar and R. Manetsch, *Synth. Commun.*, 2018, **48**, 626–631.
52 Y. Tamura, J. Minamikawa, K. Sumoto, S. Fujii and M. Ikeda, *J. Org. Chem.*, 1973, **38**, 1239–1241.
53 T. Jack, M. D. Ruepp, A. J. Thompson, O. Mühlemann and M. Lochner, *Chimia*, 2014, **68**, 239–242.
54 T. Mayer and M. E. Maier, *Eur. J. Org. Chem.*, 2007, 4711–4720.
55 Y. Hatanaka, M. Hashimoto, H. Kurihara, H. Nakayama and Y. Kanaoka, *J. Org. Chem.*, 1994, **59**, 383–387.
56 K. Fang, M. Hashimoto, S. Jockusch, N. J. Turro and K. Nakanishi, *J. Am. Chem. Soc.*, 1998, **120**, 8543–8544.
57 A. Ishida, L. Wang, Z. P. Tachrim, T. Suzuki, Y. Sakihama, Y. Hashidoko and M. Hashimoto, *ChemistrySelect*, 2017, **2**, 160–164.

58 T. Wixe and F. Almqvist, *Tetrahedron Lett.*, 2017, **58**, 3350–3352.
59 L. Wang, T. Yoshida, Y. Muto, Y. Murai, Z. P. Tachrim, A. Ishida, S. Nakagawa, Y. Sakihama, Y. Hashidoko, K. Masuda, Y. Hatanaka and M. Hashimoto, *Eur. J. Org. Chem.*, 2015, 3129–3134.
60 N. S. Kumar and R. N. Young, *Bioorg. Med. Chem.*, 2009, **17**, 5388–5395.
61 F. M. Richards, R. Lamed, R. Wynn, D. Patel and G. Olack, *Protein Sci.*, 2000, **9**, 2506–2517.
62 P. O. Craig, D. B. Ureta and J. M. Delfino, *Protein Sci.*, 2002, **11**, 1353–1366.
63 D. B. Ureta, P. O. Craig, G. E. Gómez and J. M. Delfino, *Biochemistry*, 2007, **46**, 14567–14577.
64 Z. Li, P. Hao, L. Li, C. Y. J. Tan, X. Cheng, G. Y. J. Chen, S. K. Sze, H. M. Shen and S. Q. Yao, *Angew. Chem., Int. Ed.*, 2013, **52**, 8551–8556.
65 Z. Li, D. Wang, L. Li, S. Pan, Z. Na, C. Y. J. Tan and S. Q. Yao, *J. Am. Chem. Soc.*, 2014, **136**, 9990–9998.
66 S. Pan, S. Y. Jang, D. Wang, S. S. Liew, Z. Li, J. S. Lee and S. Q. Yao, *Angew. Chem., Int. Ed. Engl.*, 2017, **56**, 11816–11821.
67 J. Gao, A. Mfuh, Y. Amako and C. M. Woo, *J. Am. Chem. Soc.*, 2018, **140**, 4259–4268.
68 L. Wang, Z. P. Tachrim, N. Kurokawa, F. Ohashi, Y. Sakihama, Y. Hashidoko and M. Hashimoto, *Molecules*, 2017, **22**, 1389.
69 J. R. Hill and A. A. B. Robertson, *J. Med. Chem.*, 2018, DOI: 10.1021/acs.jmedchem.7b01561.
70 D. P. Murale, S. C. Hong, M. M. Haque and J. S. Lee, *Proteome Sci.*, 2016, **15**, 14.
71 M. Suchanek, A. Radzikowska and C. Thiele, *Nat. Methods*, 2005, **2**, 261–268.
72 K. Markham, Y. Bai and G. Schmitt-Ulms, *Anal. Bioanal. Chem.*, 2007, **389**, 461–473.
73 M. Vila-Perelló, M. R. Pratt, F. Tulin and T. W. Muir, *J. Am. Chem. Soc.*, 2007, **129**, 8068–8069.
74 A. L. MacKinnon, J. L. Garrison, R. S. Hegde and J. Taunton, *J. Am. Chem. Soc.*, 2007, **129**, 14560–14561.
75 B. Häupl, C. H. Ihling and A. Sinz, *Proteomics*, 2017, **17**, 1600459.
76 N. Lipstein, M. Göth, C. Piotrowski, K. Pagel, A. Sinz and O. Jahn, *Expert Rev. Proteomics*, 2017, **14**, 223–242.
77 N. Srinivas, P. Jetter, B. J. Ueberbacher, M. Werneburg, K. Zerbe, J. Steinmann, B. Van der Meijden, F. Bernardini, A. Lederer, R. L. Dias, P. E. Misson, H. Henze, J. Zumbrunn, F. O. Gombert, D. Obrecht, P. Hunziker, S. Schauer, U. Ziegler, A. Kach, L. Eberl, K. Riedel, S. J. DeMarco and J. A. Robinson, *Science*, 2010, **327**, 1010–1013.
78 K. Zerbe, K. Moehle and J. A. Robinson, *Acc. Chem. Res.*, 2017, **50**, 1323–1331.
79 M. Urfer, J. Bogdanovic, F. Lo Monte, K. Moehle, K. Zerbe, U. Omasits, C. H. Ahrens, G. Pessi, L. Eberl and J. A. Robinson, *J. Biol. Chem.*, 2016, **291**, 1921–1932.
80 M. H. Wright, C. Fetzer and S. A. Sieber, *J. Am. Chem. Soc.*, 2017, **139**, 6152–6159.
81 M. Nassal, *J. Am. Chem. Soc.*, 1984, **106**, 7540–7545.
82 H. Nakashima, M. Hashimoto, Y. Sadakane, T. Tomohiro and Y. Hatanaka, *J. Am. Chem. Soc.*, 2006, **128**, 15092–15093.
83 E. M. Tippmann, W. Liu, D. Summerer, A. V. Mack and P. G. Schultz, *ChemBioChem*, 2007, **8**, 2210–2214.
84 N. Hino, M. Oyama, A. Sato, T. Mukai, F. Iraha, A. Hayashi, H. Kozuka-Hata, T. Yamamoto, S. Yokoyama and K. Sakamoto, *J. Mol. Biol.*, 2011, **406**, 343–353.
85 Y. Yang, H. Song and P. R. Chen, *IUBMB Life*, 2016, **68**, 879–886.
86 K. Masuda, A. Koizumi, T. Misaka, Y. Hatanaka, K. Abe, T. Tanaka, M. Ishiguro and M. Hashimoto, *Bioorg. Med. Chem. Lett.*, 2010, **20**, 1081–1083.
87 Y. Murai, K. Masuda, Y. Sakihama, Y. Hashidoko, Y. Hatanaka and M. Hashimoto, *J. Org. Chem.*, 2012, **77**, 8581–8587.
88 T. Wartmann and T. Lindel, *Eur. J. Org. Chem.*, 2013, 1649–1652.
89 C. Chou, R. Uprety, L. Davis, J. W. Chin and A. Deiters, *Chem. Sci.*, 2011, **2**, 480–483.
90 T. Yang, X. M. Li, X. Bao, Y. M. Fung and X. D. Li, *Nat. Chem. Biol.*, 2016, **12**, 70–72.
91 X. Xie, X. M. Li, F. Qin, J. Lin, G. Zhang, J. Zhao, X. Bao, R. Zhu, H. Song, X. D. Li and P. R. Chen, *J. Am. Chem. Soc.*, 2017, **139**, 6522–6525.
92 M. Taranenko, M. Mtchedlidze, N. Sumbatyan and G. Korshunova, *Nucleosides, Nucleotides Nucleic Acids*, 2003, **22**, 715–717.
93 U. K. Shigdel, J. Zhang and C. He, *Angew. Chem., Int. Ed. Engl.*, 2008, **47**, 90–93.
94 Z. Qiu, L. Lu, X. Jian and C. He, *J. Am. Chem. Soc.*, 2008, **130**, 14398–14399.
95 M. Winnacker, S. Breeger, R. Strasser and T. Carell, *ChemBioChem*, 2009, **10**, 109–118.
96 M. Winnacker, V. Welzmiller, R. Strasser and T. Carell, *ChemBioChem*, 2010, **11**, 1345–1349.
97 P. V. Sergiev, I. N. Lavrik, V. A. Wlasoff, S. S. Dokudovskaya, O. A. Dontsova, A. A. Bogdanov and R. Brimacombe, *RNA*, 1997, **3**, 464–475.
98 P. Sergiev, S. Dokudovskaya, E. Romanova, A. Topin, A. Bogdanov, R. Brimacombe and O. Dontsova, *Nucleic Acids Res.*, 1998, **26**, 2519–2525.
99 I. N. Lavrik, P. V. Sergive, A. A. Bogdanov, R. A. Zimmermann and O. A. Dontsova, *Molecular Biology*, 2004, **38**, 799–805.
100 S. Kuboe, M. Yoda, A. Ogata, Y. Kitade, Y. Tomari and Y. Ueno, *Chem. Commun.*, 2010, **46**, 7367–7369.
101 K. Nakamoto and Y. Ueno, *J. Org. Chem.*, 2014, **79**, 2463–2472.
102 K. Nakamoto, K. Minami, Y. Akao and Y. Ueno, *Chem. Commun.*, 2016, **52**, 6720–6722.
103 F. Muttach, F. Mäsing, A. Studer and A. Rentmeister, *Chem.–Eur. J.*, 2017, **23**, 5988–5993.
104 B. Erni and H. G. Khorana, *J. Am. Chem. Soc.*, 1980, **102**, 3888–3896.
105 J. Brunner, *Annu. Rev. Biochem.*, 1993, **62**, 483–514.

106 A. H. Ross, R. Ramachandran, R. J. Robson and H. G. Khorana, *J. Biol. Chem.*, 1982, **257**, 4152–4161.
107 T. Stegmann, J. M. Delfino, F. M. Richards and A. Helenius, *J. Biol. Chem.*, 1991, **266**, 18404–18410.
108 M. J. F. W. Janssen, F. van Voorst, G. E. J. Ploeger, P. M. Larsen, M. R. Larsen, A. I. P. M. de Kroon and B. de Kruijff, *Biochemistry*, 2002, **41**, 5702–5711.
109 P. Haberkant, O. Schmitt, F. X. Contreras, C. Thiele, K. Hanada, H. Sprong, C. Reinhard, F. T. Wieland and B. Brügger, *J. Lipid Res.*, 2008, **49**, 251–262.
110 P. Haberkant, F. Stein, D. Höglinger, M. J. Gerl, B. Brugger, P. P. Van Veldhoven, J. Krijgsveld, A. C. Gavin and C. Schultz, *ACS Chem. Biol.*, 2016, **11**, 222–230.
111 P. Haberkant, R. Raijmakers, M. Wildwater, T. Sachsenheimer, B. Brügger, K. Maeda, M. Houweling, A. C. Gavin, C. Schultz, G. van Meer, A. J. Heck and J. C. Holthuis, *Angew. Chem., Int. Ed. Engl.*, 2013, **52**, 4033–4038.
112 D. Höglinger, A. Nadler, P. Haberkant, J. Kirkpatrick, M. Schifferer, F. Stein, S. Hauke, F. D. Porter and C. Schultz, *Proc. Natl. Acad. Sci. U. S. A.*, 2017, **114**, 1566–1571.
113 X. Liu, T. Dong, Y. Zhou, N. Huang and X. Lei, *Angew. Chem., Int. Ed.*, 2016, **55**, 14330–14334.
114 X. Gu, Y. Huang, B. S. Levison, G. Gerstenecker, A. J. DiDonato, L. B. Hazen, J. Lee, V. Gogonea, J. A. DiDonato and S. L. Hazen, *J. Biol. Chem.*, 2016, **291**, 1890–18904.
115 D. Wang, S. Du, A. Cazenave-Gassiot, J. Ge, J. S. Lee, M. R. Wenk and S. Q. Yao, *Angew. Chem., Int. Ed.*, 2017, **56**, 5829–5833.
116 K. Sakurai, *Asian J. Org. Chem.*, 2015, **4**, 116–126.
117 C. R. Bertozzi and L. L. Kiessling, *Science*, 2001, **291**, 2357–2364.
118 C. S. Kuhn, J. Lehmann, G. Jung and S. Stevanović, *Carbohydr. Res.*, 1992, **232**, 227–233.
119 C. S. Kuhn, J. Lehmann and K. Sandhoff, *Bioconjugate Chem.*, 1992, **3**, 230–233.
120 B. Liessem, G. J. Glombitza, F. Knoll, J. Lehmann, J. Kellermann, F. Lottspeich and K. Sandhoff, *J. Biol. Chem.*, 1995, **270**, 23693–23699.
121 J. E. McCombs, C. Zou, R. B. Parker, C. W. Cairo and J. J. Kohler, *ACS Chem. Biol.*, 2016, **11**, 185–192.
122 Y. Tanaka and J. J. Kohler, *J. Am. Chem. Soc.*, 2008, **130**, 3278–3279.
123 M. R. Bond, H. Zhang, P. D. Vu and J. J. Kohler, *Nat. Protoc.*, 2009, **4**, 1044–1063.
124 S. H. Yu, M. Boyce, A. M. Wands, M. R. Bond, C. R. Bertozzi and J. J. Kohler, *Proc. Natl. Acad. Sci. U. S. A.*, 2012, **109**, 4834–4839.
125 M. R. Bond, H. Zhang, J. Kim, S. H. Yu, F. Yang, S. M. Patrie and J. J. Kohler, *Bioconjugate Chem.*, 2011, **22**, 1811–1823.
126 K. Sakurai, S. Ozawa, R. Yamada, T. Yasui and S. Mizuno, *ChemBioChem*, 2014, **15**, 1399–1403.
127 K. Sakurai, T. Yasui and S. Mizuno, *Asian J. Org. Chem.*, 2015, **4**, 724–728.
128 M. J. Monte, J. J. Marin, A. Antelo and J. Vazquez-Tato, *World J. Gastroenterol.*, 2009, **15**, 804–816.
129 W. Kramer and G. Kurz, *J. Lipid Res.*, 1983, **24**, 910–923.
130 P. von Dippe and D. Levy, *J. Biol. Chem.*, 1983, **258**, 8896–8901.
131 W. Kramer and S. Schneider, *J. Lipid Res.*, 1989, **30**, 1281–1288.
132 S. Zhuang, Q. Li, L. Cai, C. Wang and X. Lei, *ACS Cent. Sci.*, 2017, **3**, 501–509.
133 C. Thiele, M. J. Hannah, F. Fahrenholz and W. B. Huttner, *Nat. Cell Biol.*, 2000, **2**, 42–49.
134 M. Suchanek, R. Hynynen, G. Wohlfahrt, M. Lehto, M. Johansson, H. Saarinen, A. Radzikowska, C. Thiele and V. M. Olkkonen, *Biochem. J.*, 2007, **405**, 473–480.
135 J. C. Cruz, M. Thomas, E. Wong, N. Ohgami, S. Sugii, T. Curphey, C. C. Y. Chang and T. Y. Chang, *J. Lipid Res.*, 2002, **43**, 1341–1347.
136 N. Ohgami, D. C. Ko, M. Thomas, M. P. Scott, C. C. Y. Chang and T. Y. Chang, *Proc. Natl. Acad. Sci. U. S. A.*, 2004, **101**, 12473–12478.
137 J. J. Hulce, A. B. Cognetta, M. J. Niphakis, S. E. Tully and B. F. Cravatt, *Nat. Methods*, 2013, **10**, 259–264.
138 R. Darbandi-Tonkabon, W. R. Hastings, C. M. Zeng, G. Akk, B. D. Manion, J. R. Bracamontes, J. H. Steinbach, S. J. Mennerick, D. F. Covey and A. S. Evers, *J. Biol. Chem.*, 2003, **278**, 13196–13206.
139 X. Jiang, H. J. Shu, K. Krishnan, M. Qian, A. A. Taylor, D. F. Covey, C. F. Zorumski and S. Mennerick, *Neuropharmacology*, 2016, **108**, 193–206.
140 P. Y. Savechenkov, D. C. Chiara, R. Desai, A. T. Stern, X. Zhou, A. M. Ziemba, A. L. Szabo, Y. Zhang, J. B. Cohen, S. A. Forman, K. W. Miller and K. S. Bruzik, *Eur. J. Med. Chem.*, 2017, **136**, 334–347.
141 M. A. Hall, J. Xi, C. Lor, S. Dai, R. Pearce, W. P. Dailey and R. G. Eckenhoff, *J. Med. Chem.*, 2010, **53**, 5667–5675.
142 P. Flood, J. Ramirez-Latorre and L. Role, *Anesthesiology*, 1997, **86**, 859–865.
143 J. M. Violet, D. L. Downie, R. C. Nakisa, W. R. Lieb and N. P. Franks, *Anesthesiology*, 1997, **86**, 866–874.
144 S. S. Jayakar, W. P. Dailey, R. G. Eckenhoff and J. B. Cohen, *J. Biol. Chem.*, 2013, **288**, 6178–6189.
145 D. S. Stewart, P. Y. Savechenkov, Z. Dostalova, D. C. Chiara, R. Ge, D. E. Raines, J. B. Cohen, S. A. Forman, K. S. Bruzik and K. W. Miller, *J. Med. Chem.*, 2011, **54**, 8124–8135.
146 G. M. S. Yip, Z. W. Chen, C. J. Edge, E. H. Smith, R. Dickinson, E. Hohenester, R. R. Townsend, K. Fuchs, W. Sieghart, A. S. Evers and N. P. Franks, *Nat. Chem. Biol.*, 2013, **9**, 715–720.
147 M. R. Ziebell, S. Nirthanan, S. S. Husain, K. W. Miller and J. B. Cohen, *J. Biol. Chem.*, 2004, **279**, 17640–17649.
148 G. D. Li, D. C. Chiara, G. W. Sawyer, S. S. Husain, R. W. Olsen and J. B. Cohen, *J. Neurosci.*, 2006, **26**, 11599–11605.
149 S. S. Husain, S. Nirthanan, D. Ruesch, K. Solt, Q. Cheng, G. D. Li, E. Arevalo, R. W. Olsen, D. E. Raines, S. A. Forman, J. B. Cohen and K. W. Miller, *J. Med. Chem.*, 2006, **49**, 4818–4825.

150 S. S. Husain, D. Stewart, R. Desai, A. K. Hamouda, S. G. Li, E. Kelly, Z. Dostalova, X. Zhou, J. F. Cotten, D. E. Raines, R. W. Olsen, J. B. Cohen, S. A. Forman and K. W. Miller, *J. Med. Chem.*, 2010, **53**, 6432–6444.
151 S. Nirthanan, G. Chiara III, D. C. Chiara, S. S. Husain and J. B. Cohen, *J. Biol. Chem.*, 2008, **283**, 22051–22062.
152 M. J. Evans and B. F. Cravatt, *Chem. Rev.*, 2006, **106**, 3279–3301.
153 K. T. Barglow and B. F. Cravatt, *Nat. Methods*, 2007, **4**, 822–827.
154 M. Fonović and M. Bogyo, *Expert Rev. Proteomics*, 2008, **5**, 721–730.
155 M. Uttamchandani, J. Li, H. Sun and S. Q. Yao, *ChemBioChem*, 2008, **9**, 667–675.
156 J. Dancey and E. A. Sausville, *Nat. Rev. Drug Discovery*, 2003, **2**, 296–313.
157 M. W. Karaman, S. Herrgard, D. K. Treiber, P. Gallant, C. E. Atteridge, B. T. Campbell, K. W. Chan, P. Ciceri, M. I. Davis, P. T. Edeen, R. Faraoni, M. Floyd, J. P. Hunt, D. J. Lockhart, Z. V. Milanov, M. J. Morrison, G. Pallares, H. K. Patel, S. Pritchard, L. M. Wodicka and P. P. Zarrinkar, *Nat. Biotechnol.*, 2008, **26**, 127–132.
158 H. Shi, X. Cheng, S. K. Sze and S. Q. Yao, *Chem. Commun.*, 2011, **47**, 11306–11308.
159 H. Shi, C. J. Zhang, G. Y. J. Chen and S. Q. Yao, *J. Am. Chem. Soc.*, 2012, **134**, 3001–3014.
160 Y. Su, S. Pan, Z. Li, L. Li, X. Wu, P. Hao, S. K. Sze and S. Q. Yao, *Sci. Rep.*, 2015, **5**, 7724.
161 P. Kleiner, W. Heydenreuter, M. Stahl, V. S. Korotkov and S. A. Sieber, *Angew. Chem., Int. Ed.*, 2016, **56**, 1396–1401.
162 J. Das, G. H. Addona, W. S. Sandberg, S. S. Husain, T. Stehle and K. W. Miller, *J. Biol. Chem.*, 2004, **279**, 37964–37972.
163 J. Das, X. Zhou and K. W. Miller, *Protein Sci.*, 2006, **15**, 2107–2119.
164 G. H. Addona, S. S. Husain, T. Stehle and K. W. Miller, *J. Biol. Chem.*, 2002, **277**, 25685–25691.
165 M. Hashimoto, K. Nabeta and K. Murakami, *Bioorg. Med. Chem. Lett.*, 2003, **13**, 1531–1533.
166 A. Saito, K. Kawai, H. Takayama, T. Sudo and H. Osada, *Chem.–Asian J.*, 2008, **3**, 1607–1612.
167 Z. Y. Wang, H. Seto, S. Fujioka, S. Yoshida and J. Chory, *Nature*, 2001, **410**, 380–383.
168 T. Kinoshita, A. Caño-Delgado, H. Seto, S. Hiranuma, S. Fujioka, S. Yoshida and J. Chory, *Nature*, 2005, **433**, 167–171.
169 P. Ranjitkar, B. G. Perera, D. L. Swaney, S. B. Hari, E. T. Larson, R. Krishnamurty, E. A. Merritt, J. Villén and D. J. Maly, *J. Am. Chem. Soc.*, 2012, **134**, 19017–19025.
170 S. E. Eni, M. Rowland and M. D. Best, *RSC Adv.*, 2015, **5**, 25457–25461.
171 H. F. Dovey, V. John, J. P. Anderson, L. Z. Chen, P. de Saint Andrieu, L. Y. Fang, S. B. Freedman, B. Folmer, E. Goldbach, E. J. Holsztynska, K. L. Hu, K. L. Johnson-Wood, S. L. Kennedy, D. Kholodenko, J. E. Knops, L. H. Latimer, M. Lee, Z. Liao, I. M. Lieberburg, R. N. Motter, L. C. Mutter, J. Nietz, K. P. Quinn, K. L. Sacchi, P. A. Seubert, G. M. Shopp, E. D. Thorsett, J. S. Tung, J. Wu, S. Yang, C. T. Yin, D. B. Schenk, P. C. May, L. D. Altstiel, M. H. Bender, L. N. Boggs, T. C. Britton, J. C. Clemens, D. L. Czilli, D. K. Dieckman-McGinty, J. J. Droste, K. S. Fuson, B. D. Gitter, P. A. Hyslop, E. M. Johnstone, W. Y. Li, S. P. Little, T. E. Mabry, F. D. Miller and J. E. Audia, *J. Neurochem.*, 2001, **76**, 173–181.
172 H. Fuwa, Y. Takahashi, Y. Konno, N. Watanabe, H. Miyashita, M. Sasaki, H. Natsugari, T. Kan, T. Fukuyama, T. Tomita and T. Iwatsubo, *ACS Chem. Biol.*, 2007, **2**, 408–418.
173 C. J. Crump, S. V. Castro, F. Wang, N. Pozdnyakov, T. E. Ballard, S. S. Sisodia, K. R. Bales, D. S. Johnson and Y. M. Li, *Biochemistry*, 2012, **51**, 7209–7211.
174 C. J. Crump, H. E. Murrey, T. E. Ballard, C. W. Am Ende, X. Wu, N. Gertsik, D. S. Johnson and Y. M. Li, *ACS Chem. Neurosci.*, 2016, **7**, 1166–1173.
175 A. Rennhack, T. Jumpertz, J. Ness, S. Baches, C. U. Pietrzik, S. Weggen and B. Bulic, *Bioorg. Med. Chem.*, 2012, **20**, 6523–6532.
176 T. Jumpertz, A. Rennhack, J. Ness, S. Baches, C. U. Pietrzik, B. Bulic and S. Weggen, *PLoS One*, 2012, **7**, e30484.
177 S. C. Lu, *Int. J. Biochem. Cell Biol.*, 2000, **32**, 391–395.
178 T. C. Petrossian and S. G. Clarke, *Mol. Cell. Proteomics*, 2011, **10**, M110.000976.
179 C. Dalhoff, M. Hüben, T. Lenz, P. Poot, E. Nordhoff, H. Koster and E. Weinhold, *ChemBioChem*, 2010, **11**, 256–265.
180 B. D. Horning, R. M. Suciu, D. A. Ghadiri, O. A. Ulanovskaya, M. L. Matthews, K. M. Lum, K. M. Backus, S. J. Brown, H. Rosen and B. F. Cravatt, *J. Am. Chem. Soc.*, 2016, **138**, 13335–13343.
181 J. S. Vervacke, A. L. Funk, Y. C. Wang, M. Strom, C. A. Hrycyna and M. D. Distefano, *J. Org. Chem.*, 2014, **79**, 1971–1978.
182 B. Zhu, H. Zhang, S. Pan, C. Wang, J. Ge, J. S. Lee and S. Q. Yao, *Chem. Eur. J.*, 2016, **22**, 7824–7836.
183 C. Chang and Z. Werb, *Trends Cell Biol.*, 2001, **11**, 27–43.
184 H. D. Foda and S. Zucker, *Drug Discovery Today*, 2001, **6**, 478–482.
185 M. D. Sternlicht and Z. Werb, *Annu. Rev. Cell Dev. Biol.*, 2001, **17**, 463–516.
186 D. F. Seals and S. A. Courtneidge, *Genes Dev.*, 2003, **17**, 7–30.
187 R. A. Black and J. M. White, *Curr. Opin. Cell Biol.*, 1998, **10**, 654–659.
188 E. W. S. Chan, S. Chattopadhaya, R. C. Panicker, X. Huang and S. Q. Yao, *J. Am. Chem. Soc.*, 2004, **126**, 14435–14446.
189 M. A. Leeuwenburgh, P. P. Geurink, T. Klein, H. F. Kauffman, G. A. van der Marel, R. Bischoff and H. S. Overkleeft, *Org. Lett.*, 2006, **8**, 1705–1708.
190 P. P. Geurink, T. Klein, L. Prèly, K. Paal, M. A. Leeuwenburgh, G. A. van der Marel, H. F. Kauffman, H. S. Overkleeft and R. Bischoff, *Eur. J. Org. Chem.*, 2010, 2100–2112.
191 T. P. Lozito and R. S. Tuan, *J. Cell. Physiol.*, 2011, **226**, 385–396.

192 C. Nury, B. Czarny, E. Cassar-Lajeunesse, D. Georgiadis, S. Bregant and V. Dive, *ChemBioChem*, 2013, **14**, 107–114.
193 A. P. Wolffe, *Science*, 1996, **272**, 371–372.
194 I. V. Gregoretti, Y. M. Lee and H. V. Goodson, *J. Mol. Biol.*, 2004, **338**, 17–31.
195 C. Corminboeuf, P. Hu, M. E. Tuckerman and Y. Zhang, *J. Am. Chem. Soc.*, 2006, **128**, 4530–4531.
196 P. Gallinari, S. Di Marco, P. Jones, M. Pallaoro and C. Steinkuhler, *Cell Res.*, 2007, **17**, 195–211.
197 B. C. Smith, W. C. Hallows and J. M. Denu, *Chem. Biol.*, 2008, **15**, 1002–1013.
198 F. Hentschel, B. Raimer, G. Kelter, H. H. Fiebig, F. Sasse and T. Lindel, *Eur. J. Org. Chem.*, 2014, 2120–2127.
199 Y. Xie, J. Ge, H. Lei, B. Peng, H. Zhang, D. Wang, S. Pan, G. Chen, L. Chen, Y. Wang, Q. Hao, S. Q. Yao and H. Sun, *J. Am. Chem. Soc.*, 2016, **138**, 15596–15604.
200 Z. Liu, T. Yang, X. Li, T. Peng, H. C. Hang and X. D. Li, *Angew. Chem., Int. Ed. Engl.*, 2015, **54**, 1149–1152.
201 T. Yang, Z. Liu and X. D. Li, *Chem. Sci.*, 2015, **6**, 1011–1017.
202 T. Seifert, M. Malo, J. Lengqvist, C. Sihlbom, E. M. Jarho and K. Luthman, *J. Med. Chem.*, 2016, **59**, 10794–10799.
203 P. J. Rothwell and G. Waksman, *Adv. Protein Chem.*, 2005, **71**, 401–440.
204 T. Yamaguchi, K. Suyama, K. Narita, S. Kohgo, A. Tomikawa and M. Saneyoshi, *Nucleic Acids Res.*, 1997, **25**, 2352–2358.
205 M. Liebmann, F. Di Pasquale and A. Marx, *ChemBioChem*, 2006, **7**, 1965–1969.
206 T. Murata, I. Yamato, Y. Kakinuma, A. G. Leslie and J. E. Walker, *Science*, 2005, **308**, 654–659.
207 S. H. Lee, J. Rho, D. Jeong, J. Y. Sul, T. Kim, N. Kim, J. S. Kang, T. Miyamoto, T. Suda, S. K. Lee, R. J. Pignolo, B. Koczon-Jaremko, J. Lorenzo and Y. Choi, *Nat. Med.*, 2006, **12**, 1403–1409.
208 J. H. Kaplan, *Annu. Rev. Biochem.*, 2002, **71**, 511–535.
209 M. P. Blanton and E. A. McCardy, *Biochemistry*, 2000, **39**, 13534–13544.
210 T. Bender, M. Huss, H. Wieczorek, S. Grond and P. von Zezschwitz, *Eur. J. Org. Chem.*, 2007, 3870–3878.
211 L. C. Lo, T. L. Pang, C. H. Kuo, Y. L. Chiang, H. Y. Wang and J. J. Lin, *J. Proteome Res.*, 2002, **1**, 35–40.
212 K. Skorey, D. Waddleton, M. Therien and T. Leriche, *Anal. Biochem.*, 2006, **349**, 49–61.
213 W. T. Lowther and B. W. Matthews, *Biochim. Biophys. Acta*, 2000, **1477**, 157–167.
214 W. W. Qiu, J. Xu, J. Y. Li, J. Li and F. J. Nan, *ChemBioChem*, 2007, **8**, 1351–1358.
215 G. L. Chee, J. C. Yalowich, A. Bodner, X. Wu and B. B. Hasinoff, *Bioorg. Med. Chem.*, 2010, **18**, 830–838.
216 R. Kannappan, M. Ando, K. Furuhata and Y. Uda, *Biol. Pharm. Bull.*, 2008, **31**, 352–356.
217 A. C. Rodriguez and J. J. Kohler, *Med. Chem. Commun.*, 2014, **5**, 1227–1234.
218 R. Naik, M. Won, H. S. Ban, D. Bhattarai, X. Xu, Y. Eo, Y. S. Hong, S. Singh, Y. Choi, H. C. Ahn and K. Lee, *J. Med. Chem.*, 2014, **57**, 9522–9538.
219 N. B. Bongo, T. Tomohiro and Y. Hatanaka, *Bioorg. Med. Chem. Lett.*, 2009, **19**, 80–82.